# Large kinetic isotope effects in modern speleothems

**Patrick J. Mickler**[†]
**Libby A. Stern**[‡]
**Jay L. Banner**[§]
*Department of Geological Sciences, University of Texas, Austin, Texas 78712, USA*

## ABSTRACT

**The application of stable isotopes in speleothem records requires an understanding of the extent to which speleothem calcite isotopic compositions reflect the compositions of the cave waters from which they precipitate. To test for equilibrium precipitation, modern speleothem calcite was grown on glass plates, so that the carbon and oxygen isotope composition of the calcite and the water from which it precipitated could be directly compared. The plates were placed on the tops of three actively growing stalagmites that occupy a 1 $m^2$ area in Harrison's Cave, Barbados, West Indies. Only some of the plate $\delta^{13}C$ values and none of the plate $\delta^{18}O$ values correspond to equilibrium values, indicating significant kinetic isotope effects during speleothem calcite growth. We investigate herein mechanisms that may account for the kinetic isotope effects.**

**On each plate, speleothem calcite was deposited with distinct $\delta^{18}O$ and $\delta^{13}C$ compositions that increase progressively away from the growth axis, with up to 6.6‰ $^{13}C$ and 1.7‰ $^{18}O$ enrichments. The positive $\delta^{13}C$ versus $\delta^{18}O$ trends are likely a result of $^{18}O$ and $^{13}C$ Rayleigh-distillation enrichment in the $HCO_3^-$ reservoir owing to progressive $CO_2$ degassing and $CaCO_3$ precipitation. The magnitude of the $\delta^{13}C$ versus $\delta^{18}O$ slope is likely controlled by the extent to which $CO_2$ hydration-hydroxylation reactions buffer the oxygen isotope composition of the $HCO_3^-$ reservoir during calcite precipitation. Complete oxygen isotopic buffering of the $HCO_3^-$ reservoir by $CO_2$ hydration-hydroxylation reactions will produce a vertical $\delta^{13}C$ versus $\delta^{18}O$ slope in calcite sampled along a growth layer. As oxygen isotope buffering of the $HCO_3^-$ reservoir decreases to no buffering, the $\delta^{13}C$ versus $\delta^{18}O$ slope in calcite sampled along a growth layer will decrease from vertical to 0.52 at the cave temperature. In this study, modern speleothem calcite sampled along the growth layer produced a $\delta^{13}C$ versus $\delta^{18}O$ slope of 3.9, indicating incomplete oxygen isotope buffering of the $HCO_3^-$ reservoir during calcite precipitation.**

**Both modern and Holocene speleothem calcite from Barbados, sampled temporally along the growth axis, shows similar positive $\delta^{13}C$ versus $\delta^{18}O$ slopes. These results, along with the spatial variations in glass plate calcite carbon and oxygen isotope compositions, suggest that the isotopic composition of the Holocene speleothems is in part controlled by non-equilibrium isotope effects. In addition, there is a correlation between stalactite length and oxygen and carbon isotope ratios of calcite precipitated on the corresponding stalagmite and glass plate, which may be due to $^{13}C$ and $^{18}O$ enrichment of the $HCO_3^-$ reservoir during $CO_2$ degassing–calcite precipitation along the overhanging stalactite.**

**We compiled 165 published speleothem stable isotope records with a global distribution and found that most of these records show a positive covariation between $\delta^{13}C$ and $\delta^{18}O$ values. Speleothem stable isotope records may be influenced by kinetic isotope effects such that temperature-controlled equilibrium fractionation models alone cannot directly explain the significance of the variations in these records. Advancing the interpretation of these records requires the calibration of cave environmental conditions with the non-equilibrium isotope effects that cause $\delta^{13}C$ and $\delta^{18}O$ covariations in speleothems.**

**Keywords: kinetic isotope effects, speleothems, oxygen isotopes, carbon isotopes, non-equilibrium, Barbados.**

## INTRODUCTION

The geochemistry of speleothems, which are secondary mineral deposits formed in caves, can be used to infer past environmental conditions. Speleothems have the potential to be a powerful tool in climatic studies because (1) the isotopic and chemical compositions of speleothems record temporal changes in groundwater chemistry that may be controlled by environmental conditions (Hendy, 1971; Banner et al., 1996; Bar-Matthews et al., 2000), (2) speleothems are commonly deposited continuously over thousands of years and can be placed into a precise chronostratigraphy using U-series dating techniques (Edwards et al., 1987; Musgrove et al., 2001), and (3) speleothems can form in low altitude, low-latitude terrestrial environments for which other high-resolution climatic records may be scarce. These factors can combine to produce a long, continuous high-resolution record of terrestrial climate change.

The oxygen and carbon isotopic compositions of calcite speleothems, particularly stalagmites, are of interest to paleoclimate researchers. $\delta^{18}O$ variations in speleothems have been used to infer: (1) temporal changes in cave temperature, which is approximately equivalent to the mean annual temperature outside the cave environment (Hendy, 1971); (2) an average $\delta^{18}O$ value of precipitation (Hellstrom et al., 1998), which may reflect ice volume, temperature of condensation, the seasonality of precipitation, the "amount effect," and sources of water vapor (Dansgaard, 1964; Harmon et al., 1978b); and (3) the extent of evaporation in the vadose zone (Lauritzen and Lundberg, 1999; McDermott, 2004). $\delta^{13}C$ variations in speleothems have been used to infer the relative proportions of $C_3$ versus $C_4$ plants that control the $\delta^{13}C$ value of soil-respired $CO_2$ (Holmgren et al., 1995), changes in ecosystem productivity that control soil $P_{CO_2}$ (Genty et al., 2003), changes in the $\delta^{13}C$ value of atmospheric $CO_2$ (Baskaran and Krishnamurthy, 1993), and changes in water-rock interactions (see review by McDermott, 2004). More detailed explanations that outline the interpretations of stable isotope variations in speleothems in climatic studies can be found in Hendy (1971), Gascoyne (1992), Lauritzen

[†]E-mail: mickler@email.unc.edu.
[‡]E-mail: lstern@mail.utexas.edu.
[§]E-mail: banner@mail.utexas.edu.

*GSA Bulletin*; January/February 2006; v. 118; no. 1/2; p. 65–81; doi: 10.1130/B25698.1; 7 figures; 4 tables.

(1995), Desmarchelier et al. (2000), Schwarcz (1986), and McDermott (2004). When interpreting the stable isotopic composition of speleothems, a common assumption is that calcite is precipitated in carbon and oxygen isotope equilibrium with its corresponding drip water. In our previous study, we assessed the deviation of modern speleothem calcite from carbon and oxygen isotope equilibrium along stalagmite growth axes (Mickler et al., 2004). In the present study, we further explore mechanisms for this isotopic disequilibrium by examining the detailed spatial variations in isotopic composition of speleothem calcite grown on glass plates deployed beneath cave drips.

### Tests for Isotopic Equilibrium Precipitation of Stalagmite Calcite

For temperature-dependent equilibrium fractionation factors to be used in interpreting speleothem stable isotope records, the speleothems must be precipitated in isotopic equilibrium. The following are tests for isotopic equilibrium precipitation of stalagmites. (1) $\delta^{18}O$ and $\delta^{13}C$ values of samples along a single growth layer of a stalagmite should lack a progressive increase away from the growth axis (Hendy and Wilson, 1968; Fantidis and Ehhalt, 1970; Hendy, 1971); growth-axis and growth-layer sampling schemes are shown in Figure 1A. (2) $\delta^{18}O$ and $\delta^{13}C$ values of samples taken along a single growth layer should not be positively correlated (Hendy and Wilson, 1968; Hendy, 1971; Gascoyne, 1992); the difficulty of sampling a discrete layer as it thins away from the growth axis (Linge et al., 2001a; Drysdale et al., 2004) may make resolution of the full extent of $^{13}C$ and $^{18}O$ enrichment difficult, and may produce false negative results from the application of Hendy's (1971) "test" (Dorale et al., 2002). (3) Samples taken along the growth axis should lack a positive correlation in $\delta^{18}O$ and $\delta^{13}C$ values (Goede et al., 1986; Goede, 1994; Desmarchelier et al., 2000). This last criterion is often disputed by studies that attribute the positive correlation in $\delta^{18}O$ and $\delta^{13}C$ values of calcite along the growth axis to environmental change that simultaneously affects both the $\delta^{13}C$ and $\delta^{18}O$ values of speleothems (Dorale et al., 1998; Denniston et al., 2001; Genty et al., 2003; Paulsen et al., 2003). Isotopic disequilibrium associated with rapid $CO_2$ degassing and calcite precipitation would cause speleothems to fail these three tests.

In addition to such kinetic isotope effects, environmental factors can also produce both positive and negative correlations between $\delta^{13}C$ and $\delta^{18}O$ values of speleothem growth axis calcite. Here we consider examples of carbon and oxygen isotope variations produced by four climatic regimes.

1. In tropical and monsoonal climates, the amount effect is the dominant process that affects the $\delta^{18}O$ value of precipitation such that an increase in the amount of precipitation will result in precipitation with lower $\delta^{18}O$ values (Rozanski et al., 1993). This increase in precipitation amount might also cause a decrease in the $\delta^{13}C$ value of speleothem calcite by increasing soil moisture content and soil respiration rates (Raich and Schlesinger, 1992; Lachniet et al., 2004b) or by reducing water-rock interactions, thereby reducing the amount of $^{13}C$-enriched carbon derived from the host limestone (Paulsen et al., 2003), resulting in a positive correlation between the $\delta^{18}O$ and $\delta^{13}C$ values of speleothem calcite (e.g., Li et al., 2000a; Burns et al., 2002; China and southern Oman, respectively). In contrast, strong summer monsoonal rain, with low $\delta^{18}O$ values, may also favor high $\delta^{13}C$ value $C_4$ grasses (Stowe and Teeri, 1978), and we suggest that this may explain the negative correlation in $\delta^{18}O$ and $\delta^{13}C$ values of select stalagmites from Hulu Cave, Nanjing, China (Wang et al., 2001, Table 1).

2. In temperate climates, increasing temperature is correlated with higher $\delta^{18}O$ values of precipitation (Rozanski et al., 1993). Higher temperatures, however, may either decrease the $\delta^{13}C$ value of speleothem calcite by increasing soil respiration rates (Raich and Schlesinger, 1992; Genty et al., 2003) or increase the $\delta^{13}C$ value by favoring high $\delta^{13}C$ value $C_4$ plants (Stowe and Teeri, 1978; Dorale et al., 1998; Denniston et al., 2001) (i.e., positive or negative correlations).

3. In general, increased aridity may result in increased $\delta^{18}O$ values of cave drips owing to enhanced soil water evaporation (Allison, 1982) while simultaneously increasing the $\delta^{13}C$ value of speleothem calcite by any of the following: increasing productivity of $C_4$ plants (Stowe and Teeri, 1978); increasing the water stress, and thus increasing the $\delta^{13}C$ value of $C_3$ plants (Farquhar et al., 1989); and/or decreasing soil respiration rates (Raich and Schlesinger, 1992) (positive correlation).

4. Environmental change toward a dry-summer, wet-winter Mediterranean climate may decrease $\delta^{18}O$ values of average rainfall and decrease $\delta^{13}C$ values of soil-respired $CO_2$ by decreasing the proportion of $C_4$ plants that grow

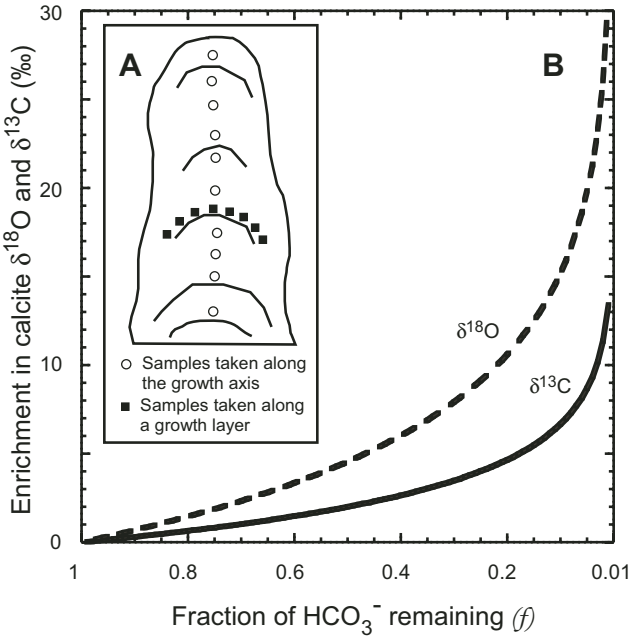


**Figure 1. (A) Schematic diagram of a stalagmite, showing the geometry of samples taken along a growth axis (open circles) and samples taken along a growth layer (filled squares). (B) Rayleigh distillation model of $\delta^{13}C$ and $\delta^{18}O$ values of $CaCO_3$ during progressive $CO_2$ degassing and $CaCO_3$ precipitation, as monitored by the fraction of $HCO_3^-$ remaining in a drip water (i.e., *f* term in equation 2). Note the progressive increase in calcite $\delta^{13}C$ and $\delta^{18}O$ values as $CO_2$ degassing and calcite precipitation proceeds. Limitations on the model prediction owing to uncertainties in the effects of $CO_2$ hydration-dehydration reactions on the extent of oxygen isotope exchange between dissolved inorganic carbon (DIC) and water are discussed in the text.**

TABLE 1. CARBON AND OXYGEN ISOTOPE TRENDS AND STUDY AREA CHARACTERISTICS OF PUBLISHED SPELEOTHEM RECORDS, LISTED BY GEOGRAPHIC REGION

| References | Speleothem name | Sample type[†] | Slope[‡] | $R^2$[§] | Number of analyses | Age range (ka) | G.R.[#] (cm/ka) | T. (°C) | Elev. (m) | Location |
|---|---|---|---|---|---|---|---|---|---|---|
| North America | | | | | | | | | | |
| Denniston et al. (1999b)[††] | CC-A | S | 1.83 | 0.29** | 125 | 3–0 | 11 | 9 | 332 | N45° W92° |
| Denniston et al. (1999b)[††] | MC-28 | S | 0.64 | 0.54** | 109 | 7.5–0 | 4 | 8.7 | 403 | N44° W92° |
| Denniston et al. (1999b)[††] | SVC-1 | S | 1.83 | 0.83** | 226 | 8.6–0 | 7.5 | 8 | 397 | N44° W92° |
| Denniston et al. (1999b)[††] | SVC-2 | S | 1.12 | 0.34** | 95 | 6.6–1.8 | 11.5 | 8 | 397 | N44° W92° |
| Denniston et al. (2001) | ON-3B | S | + | | | 13.3–12.4 | 9.33 | 14 | | N38° W91° |
| Denniston et al. (1999c) | ON-3 | S | + | | | 10–2.5 | 2.66 | 14 | | N38° W91° |
| Denniston et al. (1999c) | BCC1-1 | S | + | | | 10–0 | 0.81 | 18 | | N36° W93° |
| Denniston et al. (1999a)[††] | CWC-3L | S | 3.68 | 0.07 | 291 | 8.6–2 | 4.2 | 8.8 | 320 | N43° W92° |
| Denniston et al. (1999a)[††] | CWC-2SS | S | –2.55 | 0.60** | 74 | 7.5–1 | 1.01 | 8.8 | 320 | N43° W92° |
| Denniston et al. (1999a)[††] | CWC-1S | S | 1.58 | 0.35** | 141 | 7.7–1.15 | 1.99 | 8.8 | 320 | N43° W92° |
| Dorale et al. (19980 | CC\DBL | S | + | | | 65–25 | 1.34 | | | N38° W90° |
| Dorale et al. (1998) | CC\E | S | + | | | 70–35 | 0.29 | | | N38° W90° |
| Dorale et al. (1998) | CC\C | S | X | | | 75–25 | 0.37 | | | N38° W90° |
| Gascoyne et al. (1981) | 75123 | S | X, - | | | 55–50 | | 4 | 365 | N49°W125° |
| Gascoyne et al. (1981) | 75125 | Sc-F | X | | | 64–28 | 0.23 | 4 | 365 | N49°W125° |
| Harmon et al. (1978a) | 72041 | S | X | | | 230–100 | 0.22 | 13.5 | 160 | N38° W86° |
| Lauriol et al. (1997) | TITC/GB | F | 2.1 | | 8 | >350 | | [††]0 | 990 | N66°W141° |
| Lauriol et al. (1997) | TTH12-3 | F | X | | 12 | 81 | | [††]0 | 1219 | N66°W141° |
| Musgrove (2000) | IS-LM | F | 1.74 | 0.13 | 12 | 35.5–1.8 | 1.2 | 22 | | N30°W98° |
| Musgrove (2000) | ISS2 | S | 1.9 | 0.44** | 157 | 71.2–13.9 | 0.05–8 | 22 | | N30°W98° |
| Musgrove (2000) | IS-ST | F | 1.35 | 0.57 | 11 | 27.6–13.2 | 8.3 | 22 | | N30°W98° |
| Musgrove (2000) | DDS2 | S | 1.2 | 0.58** | 217 | 69.6–15.3 | 0.08–10 | | | N30°W98° |
| Musgrove (2000) | KCS2 | F | 0.84 | 0.92** | 6 | >350–29 | | | 600 | N29°W100° |
| Musgrove (2000) | KCS1 | F | 1.5 | 0.96** | 9 | >350–20.4 | 0.25 | | 600 | N29°W100° |
| Musgrove (2000) | KCS3 | F | 0.97 | 0.69* | 10 | 229.9–11.9 | 0.16 | | 600 | N29°W100° |
| Musgrove (2000) | CWN4 | S | 1.22 | 0.53** | 40 | 38.5–7.7 | 0.05–8 | 19 | | N30°W99° |
| Musgrove (2000) | NBSwall | F | 1.7 | 0.60** | 20 | 16.8–11 | 14.3 | 21 | | N30°W98° |
| Musgrove (2000) | NBSwhite | F | 4.1 | 0.84** | 10 | 11.5–8.1 | 3.9 | 21 | | N30°W98° |
| Schwehr (1998) | Tulum B | Sc | ++ | | | 0.13–0 | 196 | 26 | | N20° W87° |
| Serefiddin et al. (2004) | RC2 | S | X | | | 82–24 | 1.65 | 8 | 1400 | N44°W104° |
| Serefiddin et al. (2004) | RC20 | S-F | X | | | 62–50 | 0.22 | 8 | 1400 | N44°W104° |
| Thompson et al. (1976) | NB10 | S | X | | 44 | 200–165 | 2 | 11 | 655 | N38° W81° |
| Thompson et al. (1976) | NB11 | S | X | | 11 | 0–2 | 10 | 11 | 655 | N38° W81° |
| Thompson et al. (1976) | NB4 | S | + | | 30 | | | 11 | 655 | N38° W81° |
| Thompson et al. (1976) | GV2 | | + | | 28 | 180–145,125–62 | 0.2 | 11 | 715 | N38° W81° |
| van Beynen et al. (2004) | MF1 | S | X | | | 7.6–0 | 103–2 | 7.3 | 430 | N38°W91° |
| Caribbean/Central and South America | | | | | | | | | | |
| Cruz et al. (2005) | BT2 | S | 0.66 | 0.21** | 690 | 116.2–0 | 0.59 | | 230 | S27° W49° |
| González and Gomez (2002) | VCZ-1 | S | + | | | 12–0 | | | | N11° W70° |
| Lachniet et al. (2004b) | CHIL-1 | S | 3.99 | 0.82** | 484 | 2.184–0.696 | 33.1 | 27.1 | 60 | N9.2° W80° |
| Lachniet et al. (2004a) | V-1 | S | 2.62 | 0.68** | 297 | 8.84–5.06k | 9.15 | 25 | | N11° W85° |
| Mickler (2004) | AH-L | S | 3.3 | 0.45** | 33 | 11.6–8.4 | | 26.6 | 250 | N13° W60° |
| Mickler (2004) | AH-M | S | 2.6 | 0.88** | 20 | 93.5–66.6 | | 26.6 | 250 | N13° W60° |
| Mickler (2004) | AH-S | S | 2.1 | 0.57* | 15 | 23.1–22.1 | | 26.6 | 250 | N13° W60° |
| Mickler (2004) | BN-3 | Sc-F | 1.2 | 0.141 | 9 | 51–38 | | 26.6 | 250 | N13° W60° |
| Mickler (2004) | SH | S | 2.2 | 0.36 | 7 | 25 | | 26.6 | 250 | N13° W60° |
| Mickler (2004) | SHC | S | 4 | 0.19 | 7 | 25 | | 26.6 | 250 | N13° W60° |
| Mickler (2004) | BC-53 | S | 3.5 | 0.29 | 30 | 34.4–0 | | 26.6 | 250 | N13° W60° |
| Mickler (2004) | BC-61 | S | 2.7 | 0.70** | 46 | 53.9–0 | | 26.6 | 250 | N13° W60° |
| Europe | | | | | | | | | | |
| Bard et al. (2002) | Stalagmite I | S | X | | | 190–142 | 0.25 | 15.8 | <40m | N42° E11° |
| Drysdale et al. (2004) | CC1 | S | +,- | ** | | 43.1–383.4 | 0.05–1 | 7.5 | 1200 | N44° E10° |
| Duplessy et al. (1971) | d'Orgnac | S | X | | | 130–90 | 6 | 12.6 | | France |
| Duplessy et al. (1969) | T | S | X | | | | | 12.6 | | France |
| Duplessy et al. (1969) | G | S | 1.4 | | | | | | | France |
| Fornaca-Rinaldi et al. (1968) | Sarteano | S | X | | 41 | | | | | Italy |
| Fornaca-Rinaldi et al. (1968) | Montecello | Sc | 3.71 | 0.97** | 6 | | | | | Italy |
| Fornaca-Rinaldi et al. (1968) | S. Lucia | Sc | 6.12 | 0.89* | 6 | | | | | Italy |
| Gascoyne (1992) | 76127 | F | ++ | | | 238–225 | | | | N54° W2° |
| Gascoyne (1992) | 77143B | F | + | | | 126–108 | | | | N54° W2° |
| Gascoyne (1992) | 77162 | F | ++ | | | 114–98 | 0.75 | | | N54° W2° |

(*continued*)

TABLE 1. CARBON AND OXYGEN ISOTOPE TRENDS AND STUDY AREA CHARACTERISTICS OF PUBLISHED SPELEOTHEM RECORDS, LISTED BY GEOGRAPHIC REGION (*continued*)

| References | Speleothem name | Sample type† | Slope‡ | $R^2$§ | Number of analyses | Age range (ka) | G.R.# (cm/ka) | T. (°C) | Elev. (m) | Location |
|---|---|---|---|---|---|---|---|---|---|---|
| Gascoyne (1992) | 79151 | F-S | X,+ | | | 290–210,320–250 | 0.3 | | | N54° W2° |
| Gascoyne (1992) | 79158 | S | X | | | 180–170 | 2 | | | N54° W2° |
| Schwarcz (1986) | unnamed | S | -, + | | | 290–190 | 0.3 | | | N54° W2° |
| Genty et al. (2003)†† | Vil9 | S | 2.7 | 0.59** | 299 | 83.1–31.8 | 2.89 | 11 | | N46° E0° |
| Genty et al. (2003)†† ‡‡ | Vil9,D2- | S | 0.91 | 0.51** | 25 | 83–79 | 3.75 | 11 | | N46° E0° |
| Genty et al. (2003)†† ‡‡ | Vil9,D2-D3 | S | 1.1 | 0.58** | 61 | 76–67 | 3.11 | 11 | | N46° E0° |
| Genty et al. (2003)†† ‡‡ | Vil9,D3-D4 | S | 3.4 | 0.50** | 40 | 61–56 | 2.05 | 11 | | N46° E0° |
| Genty et al. (2003)†† ‡‡ | Vil9,D4-D6 | S | 1.9 | 0.63** | 127 | 52–40 | 7.4 | 11 | | N46° E0° |
| Genty et al. (2003)†† ‡‡ | Vil9,D6- | S | 2.7 | 0.61** | 46 | 40–32 | 0.99 | 11 | | N46° E0° |
| Genty et al. (1998) | Han-stm5b | S | 1.2 | 0.35 | 10 | 0.045–0 | 8.8 | 8.9 | 180 | N50° E5° |
| Gewelt (1981) | RSM V | S | 1.3 | 0.33 | 15 | 11–5 | | 9 | | N50° E5° |
| Horvatinčić et al. (2003) | Pos CG-85 | S | 0.43 | 0.83** | 10 | Holocene | | 8 | 529 | N46° E14° |
| Jiménez de Cisneros et al. (2003) | ET | Sc | 2.2 | 0.94** | 18 | 190–160 | | 20 | | N37° W4° |
| Kacanski et al. (2001) | Cermosjna | S | 3.8 | 0.81 | 5 | 2.3–0 | 6.36 | 11.6 | 530 | N45° E21° |
| Kadlec et al. (1996) | Zazdĭná | F | X | | | 100, 124–114.4 | | | | |
| Kadlec et al. (1996) | Holstenjnšká | F | 1.2 | | | 114.4 to 99.9 | | | | |
| Labonne et al. (2002) | Altamira | F | X | | | 22–10.7 | 2.2 | 18 | | N42° E3° |
| Lauritzen and Onac (1999) | LFG-2 | S | X | | | 131–58 | 0.67 | | 545 | N47° E23° |
| Lauritzen and Lundberg (2004) | LP6 | F | + | | | 424–392 | 0.25–0.66 | | | N66° E14° |
| Lauritzen (1995) | S-88-17 | F | + | | | 118–6 | 3.5 | | 920 | N68° E16° |
| Lauritzen (1995)‡‡ | S-88-17seg1 | F | ++ | | | 8–6 | 3.5 | | 920 | N68° E16° |
| Lauritzen (1995)‡‡ | S-88-17seg2 | F | +,X | | | 118–106 | | | 920 | N68° E16° |
| Lauritzen (1995) | FM-2 | F | 2.9 | ++ | | 145–80 | 0.21 | | 160 | N67° E14° |
| Linge et al. (2001a) | FM3 | | 5.6 | | | | 3.41 | | 160 | N67° E14° |
| Linge et al. (2001a) | L-03 | | 3.4 | | | 200 | | | | N66° E13° |
| Linge et al. (2001a) | Ham85-2 | S | + | | | 123–73 | 4.6 | 3.5 | 220 | |
| Linge et al. (2001a) | SG92-1 | | X | | | Eemian | | 2.8 | 280 | N67° E13° |
| Linge et al. (2001b) | SG93 | S | - + | | | 140–10 | | 2.8 | 280 | N67° E13° |
| Linge et al. (2001b) | SG95 | S | X | | | 4.2–0 | 3.46 | 2.8 | 280 | N67° E13° |
| Linge et al. (2001b) | SG92-4 | S | + | | | 8–4.5 | | 2.8 | 280 | N67° E13° |
| Berstad et al. (2002)††† | SG92-2 | S | 3.64 | 0.50** | 232 | 630–330 | 0.08 | 2.8 | 280 | N67° E13° |
| McDermott et al. (1999) | ER76 | S | X | | | 12–0 | 4 | 6.6 | 1165 | N45°E12° |
| McDermott et al. (1999) | CC3 | S | X | | | 9–0 | 4.04 | 10.4 | 60 | N52° W9° |
| McDermott et al. (1999) | CL26 | S | X | | | 11.5–0 | 4.3 | 14.5 | 75 | N44° E4° |
| Plagnes et al. (2002) | Cla4 | S | 2.4 | 0.73** | 75 | 189–74 | 0.2–10 | 14.5 | 75 | N44° E4° |
| Plagnes et al. (2002)‡‡ | Cla4A | S | 4.7 | 0.67* | 11 | 75.7–74.5 | 6 | 14.5 | 75 | N44° E4° |
| Plagnes et al. (2002)‡‡ | Cla4B | S | 8 | 0.22 | 21 | 83.4–82.4 | 20 | 14.5 | 75 | N44° E4° |
| Plagnes et al. (2002)‡‡ | Cla4C | S | 10 | 0.2 | 10 | 112.5–99.1 | 0.2 | 14.5 | 75 | N44° E4° |
| Plagnes et al. (2002)‡‡ | Cla4D | S | –-5 | 0.35 | 15 | 128–118 | 3 | 14.5 | 75 | N44° E4° |
| Plagnes et al. (2002)‡‡ | Cla4E | S | 2.9 | 0.92** | 10 | 170–160 | 1 | 14.5 | 75 | N44° E4° |
| Plagnes et al. (2002)‡‡ | Cla4F | S | –4 | 0.44 | 8 | 189–188 | 10 | 14.5 | 75 | N44° E4° |
| Niggemann et al. (2003b) | Stal-B7-1 | S | >1 | 0.63** | 98 | 12.5–6 | 12.5–6 | 9.4 | 185 | N49° E7° |
| Niggemann et al. (2003b) | Stal-B7-5 | S | >1 | 0.55** | 50 | 9–5.5 | 9–5.5 | 9.4 | 185 | N49° E7° |
| Niggemann et al. (2003b) | Stal-B7-7 | S | >1 | 0.63** | 228 | 18–17,9.5–5,2.2–0 | 1.8–26 | 9.4 | 185 | N49° E7° |
| Niggemann et al. (2003a) | AH-1 | S | + | 0.37** | 384 | 6–0.8 | 7.01 | 9.4 | 308 | N49° E7° |
| Onac et al. (2002) | Pu2 | S | X | | | 8–1 | 3.1 | 9.8 | 482 | N47° E23° |
| Pazdur et al. (1995) | JWi2 | S | 0.9 | 0.81** | 53 | 28–18.9 | 3.1 | 1100 | 385 | N51°E19° |
| Spötl et al. (2002) | OBI 12 | S | + | | | 8–0 | 3.9 | 5.4 | | N47°E15° |
| Verheyden et al. (2000) | Père Noël | S | + | | | 13–1.8 | 5.8 | 8.9? | 203 | N50° E5° |
| Wurth et al. (2004) | Stal-Hoel-1 | S | X,+ | | | 14.3–0 | 1.1–3.6 | 3.5 | 1440 | N47° E10° |
| Middle East | | | | | | | | | | |
| Bar-Matthews et al. (2003)†† | Peqiin | S's | 1.1 | 0.53** | 483 | 250–0Excl120–128 | | 16 | 650 | N33° E35° |
| Bar-Matthews et al. (2003)†† ‡‡ | Peqiin | S's | –1.5 | –0.27** | 568 | 250–0 | | 16 | 650 | N33° E35° |
| Bar-Matthews et al. (2003)†† ‡‡ | Peqiin | S's | 1.1 | 0.55** | 239 | 120–14 | | 16 | 650 | N33° E35° |
| Bar-Matthews et al. (2003)†† ‡‡ | Peqiin | S's | X | | | 120–131 | | 16 | 650 | N33° E35° |
| Bar-Matthews et al. (2003)†† ‡‡ | Peqiin | S's | 1.1 | 0.57** | 237 | 250–135 | | 16 | 650 | N33° E35° |
| Bar-Matthews et al. (2003)†† ‡‡ | Soreq | S's | 1.4 | 0.04 | 1387 | 184–0 | 1.5–100 | 22.5 | 400 | N31° E35° |
| Bar-Matthews et al. (2003)†† | Soreq | S's | 0.93 | 0.67** | 1340 | 184–0 Excl7–7.5, 119–128 | 1.5–100 | 22.5 | 400 | N31° E35° |
| Bar-Matthews et al. (2003)†† ‡‡ | Soreq | S's | 1.3 | 0.34** | 1149 | 118–0 | 1.5–100 | 22.5 | 400 | N31° E35° |
| Bar-Matthews et al. (2003)†† ‡‡ | Soreq | S's | –3.5 | –0.94** | 18 | 128–118 | | 22.5 | 400 | N31° E35° |
| Bar-Matthews et al. (2003)†† ‡‡ | Soreq | S's | 0.72 | 0.41** | 221 | 184–128 | | 22.5 | 400 | N31° E35° |
| Burns et al. (2002) | S3 | S | + | | | 0.740–0 | 31 | | | Oman |

(*continued*)

TABLE 1. CARBON AND OXYGEN ISOTOPE TRENDS AND STUDY AREA CHARACTERISTICS OF PUBLISHED SPELEOTHEM RECORDS, LISTED BY GEOGRAPHIC REGION (*continued*)

| References | Speleothem name | Sample type[†] | Slope[‡] | *R*[§] | Number of analyses | Age range (ka) | G.R.[#] (cm/ka) | T. (°C) | Elev. (m) | Location |
|---|---|---|---|---|---|---|---|---|---|---|
| De Geest et al. (2005) | S-Stm1 | S | 3.6 | 0.83** | | 6–0 | 1.6–23 | 29 | | N13° E54° |
| Frumkin et al. (2000)[§§] | AF12 | S | - - | | | 170–65 | 1 | 17 | 730 | N32° E35° |
| Frumkin et al. (2000)[§§] | AF12 | S | + | | | 45–0 | 2 | 17 | 730 | N32° E35° |
| Frumkin et al. (1999) | NQ38 | S | + | | | 6–0 | 4.4 | 19 | 600 | N32° E35° |
| Vaks et al. (2003)[††] | ME12+ME5 | S's | 1.4 | 0.55** | 389 | 67–16.6 | 2–100 | 21.5 | 250 | N32° E35° |
| China/Asia | | | | | | | | | | |
| Hou et al. (2003) | LS9602 | S | X | | | 1–0 | 15 | 14.5 | 200 | N40°E116° |
| Hou et al. (2003) | TS9701 | S | X | | | 2.2–0 | 8.7 | 14.5 | 200 | N40°E116° |
| Li et al. (1998b)[§§ ††† ††] | S312top | S | 1 | 0.13 | 133 | 0.486–0 | 100 | 14.5 | 200 | N40°E116° |
| Li et al. (1997)[§§] | S312 | S | –2.63 | –0.16 | 121 | 3–0 | 4.2 | 14.5 | 200 | N40°E116° |
| Tan et al. (1998) | TS9501 | S | + | 0.4** | 52 | | | 14.5 | 200 | N40°E116° |
| Huang (1992) | Shiquan | S | 2.183 | 0.2 | 8 | 16.5–3 | 1 | | | Hubei |
| Huang et al. (2001) | HS-2 | S | ++ | | | 20.2–10.5 | 5 | | 205 | N31°E111° |
| Karst-Dynamics-Laboratory | Shuinan | S | ++ | | | 190–90 | 2.46 | | | N26°E106° |
| Li et al. (1996) | Tian E | S | 1.109 | 0.34* | 48 | 220–32 | | | 430 | Fujian, China |
| Li et al. (2000b) | No 1 | S | + | | | 44–0 | 4.27 | | | N26°E106° |
| Zhang et al. (2004b) | Xiangshui | S | X | | | 6–0 | 12.44 | 19.5 | 400 | N26°E106° |
| Li et al. (1998a) | PanlongA | S | +,X | | | 35–1 | 3.4 | 19.5 | 190 | N39°E115° |
| Li et al. (1998a) | PanlongB | S | + | | | 30–7 | 1.2 | 19.5 | 190 | N39°E115° |
| Li et al. (1998a) | PanlongC | S | +,X | | | 30–7 | 1.2 | 19.5 | 190 | N39°E115° |
| Ma et al. (2003) | ZFFS-1 | S | + | | | 3–0 | 1 | 13 | 100 | N40°E117° |
| Paulsen et al. (2003)[§§] | SF-1seg1 | S | ++ | 0.82** | | 0.15–0 | 1.38 | 14 | 500 | N34°E109° |
| Paulsen et al. (2003)[§§] | SF-1seg2 | S | + | | | 1.23–0.15 | 1.38 | 14 | 500 | N34°E109° |
| Tsai (2002) | TSG-1 | S | 2.03 | 0.13 | 112 | 41.1–16.2 | 0.19–4.7 | | | N23°E120° |
| Tsai (2002) | TSC-1 | Sc | 1.56 | 0.08 | 30 | 13.5–9.0 | 0.3–3.4 | | | N23°E120° |
| Tsai (2002) | GS | Sc | 8.1 | 0.25 | 20 | 165–13 | 0.01–0.2 | | | N25°E121° |
| Wang (1986) | 82-29 | S | + | | 6 | >350–112 | | | 250 | |
| Wang (1986) | GL | S | + | | 16 | 385–267 | 2.7 | | 250 | |
| Wang et al. (2001)[†† ‡‡ ##] | Composite | S | –0.13 | –0.10** | 1652 | 75–11 | | 15.4 | 80 | N32°E119° |
| Wang et al. (2001)[†† ##] | MSD | S | –1.23 | –0.79** | 268 | 54–19 | 1 | 15.4 | 80 | N32°E119° |
| Wang et al. (2001)[†† ##] | MSL | S | –-1.93 | –0.62** | 285 | 75–31 | 1.16 | 15.4 | 80 | N32°E119° |
| Wang et al. (2001)[†† ##] | PD | S | 1 | 0.53** | 149 | 19–11 | 0.84 | 15.4 | 80 | N32°E119° |
| Wang et al. (2001)[†† ##] | YT | S | –0.42 | –0.48** | 338 | 17–14.5 | 4.1 | 15.4 | 80 | N32°E119° |
| Wang et al. (2000)[##] | MS-1 | S | 5.102 | 0.59** | 82 | 463–159 | 0.027 | 15.4 | 80 | N32°E119° |
| Yuan et al. (2004)[†† ##] | H82 | S | 3.22 | 0.35** | 833 | 16–11 | 1.1–5 | 15.4 | 80 | N32°E119° |
| Wang et al. (1998)[##] | Hulu | S | + | | 32 | 380–170 | 0.34 | 15.4 | 80 | N32°E119° |
| Zhao et al. (2003)[##] | 996182 | S | X | | | 17–10 | | 15.4 | 80 | N32°E119° |
| Wang et al. (1995) | BZ4 | S | + | 0.68* | 9 | 76–55 | 1.1 | | | near Bejing |
| Wang et al. (1995) | BZ4' | S | + | 0.36 | 10 | 158–74 | 0.53 | | | near Bejing |
| Wang et al. (1997) | ZL01 | S | 1.18 | 0.56 | 8 | | | | | Zhejing |
| Zhang et al. (2004a) | Q2 | S | + | | 45 | 152–122 | 7.4 | 15.8 | | N26°E108° |
| Yuan et al. (2004)[††] | D3 | S | 2.22 | 0.52** | 118 | 164–91.5 | 0.15–19 | 15.6 | 680 | N25°E108° |
| Yuan et al. (2004)[†† ‡‡] | D3* | S | 5.55 | 0.37** | 74 | <124 | 5.4 | 15.6 | 680 | N25°E108° |
| Yuan et al. (2004)[†† ‡‡] | D3* | S | 1.47 | 0.37** | 44 | >124 | 0.72 | 15.6 | 680 | N25°E108° |
| Yuan et al. (2004)[††] | D4 | S | 3.22 | 0.32** | 527 | 155–0.09 | 1.1–49 | 15.6 | 680 | N25°E108° |
| Yuan et al. (2004)[†† ‡‡] | D4* | S | 3.7 | 0.39** | 115 | <9.3 | 18 | 15.6 | 680 | N25°E108° |
| Yuan et al. (2004)[†† ‡‡] | D4* | S | 11.1 | 0.06 | 280 | 16–9.3 | 4.5 | 15.6 | 680 | N25°E108° |
| Yuan et al. (2004)[†† ‡‡] | D4* | S | 1.85 | 0.67** | 59 | 66–42 | 1.7 | 15.6 | 680 | N25°E108° |
| Yuan et al. (2004)[†† ‡‡] | D4* | S | 2.94 | 0.30** | 84 | >113 | 1.6 | 15.6 | 680 | N25°E108° |
| Yadava et al. (2004) | Akalagavi | S | ++ | 0.62** | 301 | 0.331–0 | | | | N15°E73° |
| Yadava and Ramesh (2005) | Dandak | S | 1.28 | 0.72** | 117 | 3.54–0 | 18 | 25.5 | | N19°E82° |
| Yadava and Ramesh (2005) | Gupteswar | S | 1.31 | 0.58** | 233 | 3.39–0 | 14 | 25.5 | | N19°'E82° |
| Australia/New Zealand | | | | | | | | | | |
| Desmarchelier et al. (2000) | SC-S11 | S | 1.9 | 0.77** | 90 | 190–152 | 0.83 | 16.8 | 70 | N37°E141° |
| Fischer et al. (1996) | FSDC | S | ++ | | | 55–18,2.6–0 | | | | S20°E140° |
| Goede et al. (1996) | RO | S | X+ | | | 2, 13.2–10.9 | 2.2 | 15 | 80 | S37°E148° |
| McDonald et al. (2001) | MC4 | S | + | 0.64 | | 105–88 | | | | NSW Aus. |
| Treble et al. (2005)[§§] | MND-S1 | S | 3.7 | 0.75** | 26 | 0 .075–0.050 | 12.3 | 16.2 | | S36°E115° |
| Treble et al. (2005)[§§] | MND-S1 | S | 4.5 | 0.92** | 16 | 0.095–0.076, 0.051–0.007 | 12.3 | 16.2 | | S36°E115° |
| Desmarchelier and Goede (1996) | LT | S | –1.77 | –0.4** | 119 | 110–72 | 4.05 | 9.5 | 460 | S42°E146° |
| Goede et al. (1990) | FC | S | X - | –0.19 | 36 | 4.25–2.9 | 26.7 | 8.3 | 360 | S43°E146° |

(*continued*)

TABLE 1. CARBON AND OXYGEN ISOTOPE TRENDS AND STUDY AREA CHARACTERISTICS OF PUBLISHED SPELEOTHEM RECORDS, LISTED BY GEOGRAPHIC REGION (*continued*)

| References | Speleothem name | Sample type† | Slope‡ | *R*§ | Number of analyses | Age range (ka) | G.R.# (cm/ka) | T. (°C) | Elev. (m) | Location |
|---|---|---|---|---|---|---|---|---|---|---|
| Goede (1994) | FT | S | - | –0.089 | 170 | 98–55 | 1.99 | 8.3 | 360 | S43°E146° |
| Goede and Vogel (1991) | LC | S | + | 0.73** | 40 | 15–11.7 | 22.2 | 9.5 | 300 | S42°E146° |
| Xia et al. (2001) | LYN | S | ++,X | | | 9.9–5.1 | 26.9 | 9.5 | 300 | S42°E146° |
| Hellstrom et al. (1998) | ED1 | F | + | | | 17–0 | 0.12 | 7 | 685 | S41°E173° |
| Hellstrom et al. (1998) | MD3 | F | + | | | 31–0 | 2–5 | 5 | 390 | S41°E172° |
| Williams et al. (2004) | RK-C | S | X | | | 11.0–6.1 | 5.8 | 13 | | S38°E175° |
| Williams et al. (2004) | Max's | S | X | | 56 | 6.2–2.6 | 8.9 | 11.5 | 325 | S38°E175° |
| Williams et al. (2004) | GG1 | S | X | | 42 | 9.7–0 | 3.7 | 13.3 | 100 | S38°E175° |
| Williams et al. (2004) | GG2 | S | X | | 63 | 11.8–0 | 6.5 | 13.3 | 100 | S38°E175° |
| Williams et al. (1999) | Waipuna-1 | Sc | + | 0.37** | 51 | 0.1–0 | | 11.5 | 320 | S38° |
| Africa | | | | | | | | | | |
| Holmgren et al. (1995) | LII4 | S | X | | | 51–43,38–35,28–21 | 0.86 | 20.6 | 1128 | S25° E26° |
| Holmgren et al. (2003)†† | T7 | S | 1.3 | 0.23** | 480 | 6.4–0 | 18.5 | 18 | 400 | S24° E29° |
| Holmgren et al. (2003) †† | T8 | S | 1.01 | 0.09** | 1230 | 24.4–12.7,10.2–0 | 2,11 | 18 | 400 | S24° E29° |
| Repinski et al. (1999) | T5 | S | + | | | 4.4–4,0.8–0 | 50 | 18 | 400 | S24° E29° |
| Talma and Vogel (1992) | V3 | S | X | | | 45–12,5–0 | | 17.5 | | S33° E22° |
| Talma et al. (1974) | T24 | S | -,X | | | | | 21 | 486 | S24° E30° |

†Types of speleothems are designated as: S—stalagmite; F—flowstone; Sc—stalactite; with composite stalagmite records designated S's.

‡Speleothems are designated with a slope of $\delta^{18}O$ vs. $\delta^{13}C$ (X vs. Y) graph for those studies providing either raw data, regressions, or graphs. When data were available, these slopes were determined by orthogonal regression. We categorized those speleothem studies that provide spatial or temporal variations in $\delta^{18}O$ and $\delta^{13}C$ values into five qualitative categories, corresponding to synchronous positive (+) or negative (-) covariation in $\delta^{18}O$ and $\delta^{13}C$ values, as indicated by coincident minima or maxima and overall temporal trends. Those with no apparent covariation are designated as X, and those with strong covariation are designated + + or - -. Some speleothems display discrete parts with positive, negative, or non-correlation, and are designated accordingly (e.g., +,X).

§The linear correlation coefficient, *R,* between $\delta^{18}O$ and $\delta^{13}C$ values, is designated as significant with * (>95% confidence), or highly significant with ** (>99% confidence). The lack of either * or ** indicates a correlation without rigorous significance.

#Average or range of speleothem growth rates.

††Data archived at the World Data Center for Paleoclimatology, Boulder, Colorado, USA.

‡‡Indicates parts of speleothems or composite speleothem records that are excluded from the compilation in Table 4.

§§These two segments of a single speleothem were merged as one item for Table 4.

##All of these speleothems are from the Hulu/Tangshan cave. Presumably, for an unknown environmental reason, 3 of 7 of these speleothems have negative correlations between $\delta^{18}O$ and $\delta^{13}C$ values, Table 4.

†††Excluding one outlier in regression.

best in a hot growing season, as observed in parts of speleothem records from several caves in Israel (positive correlation; e.g., Bar-Matthews et al., 1997, 1999). In contrast, Frumkin et al. (2000) invoke intense soil erosion during times of intense rainfall as the cause of negative $\delta^{13}C$ and $\delta^{18}O$ correlation during discrete intervals from these same records. The present study will show, following the theory of Hendy (1971), that a positive $\delta^{13}C$ and $\delta^{18}O$ covariation can occur from non-equilibrium isotope effects, independent of environmental changes, that result from the isotopic evolution of the dissolved inorganic carbon (DIC) reservoir during progressive $CO_2$ degassing and calcite precipitation.

## Modern Speleothems

We compare the isotopic compositions of speleothem calcite and the water from which the speleothems precipitate to assess whether calcite is precipitated in isotopic equilibrium. Modern speleothems refer here to the tips of actively growing stalagmites and to calcite grown on frosted glass plates placed on those stalagmites as substrates for calcite precipitation (Fig. 2). The spatial variations in $\delta^{18}O$ and $\delta^{13}C$ values of calcite grown on these plates are analogous to Hendy's (1971) tests 1 and 2 for isotopic equilibrium on calcite along single growth layers in ancient speleothems, with three important distinctions: (1) There is no ambiguity regarding the age of the glass plate calcite layer, because the timing of the placement and collection of the plate is precisely known. Stalagmite growth layers thin away from the growth axis, so the ability to sample the same time interval along a growth layer depends on the resolution of the sampling method. This introduces errors that increase as growth layers thin (Dorale et al., 2002). (2) Glass plate calcite can be sampled in any direction relative to the growth axis. Natural speleothems, which are commonly sliced in half, allow sampling along only one plane. (3) The carbon and oxygen isotope composition of the corresponding drip water and the temperature of formation can be measured and compared, using equilibrium isotope fractionation factors, to the carbon and oxygen isotope composition of corresponding glass plate calcite. This provides a direct test for carbon and oxygen isotope equilibrium during calcite precipitation.

## Sample Site Description

Modern speleothem calcite was sampled from the tips of three actively forming stalagmites from Harrison's Cave, Barbados. The three stalagmites studied from Harrison's Cave are in the Upper Passage (see map in Mickler et al., 2004) and occupy an area of ~1 $m^2$ (Fig. 2). We would expect that conditions in the Upper Passage sites are conducive to the precipitation of speleothems in isotopic equilibrium with their corresponding drip water relative to other locations in the cave. Speleothems at these sites form under high relative humidity (>98%; Mickler, 2004) and from relatively slow, steady drips. These conditions limit evaporative $^{18}O$ enrichment in the drip water and may limit kinetic isotope effects caused by large variations in drip rates and the accompanying changes in drip water chemistry.

All three stalagmites are ~1 m in height and of comparable diameter and are fed by drips flowing at <0.3 mL/min. However, the drips


**Figure 2. Experiment with glass plates at stalagmite sites BC-98-1, 2, and 3 in the Upper Passage of Harrison's Cave, Barbados, West Indies. Individual glass plates measure 10 cm × 10 cm.**

feeding the stalagmites originate from the tips of corresponding stalactites of different shapes and sizes (Table 2). Site BC-98-1 is fed by a bent-soda-straw stalactite ~25 cm long that thickens toward the roof of the cave. Site BC-98-2 is fed from a carrot-shaped stalactite that formed by the connection of two soda straws ~40 cm in length and 7 cm in diameter near its top. The stalactite feeding site BC-98-2 no longer has an open central cavity, and water runs down the stalactite along its outside surface. Site BC-98-3 is fed from a 7-cm-long bent soda straw, a much smaller stalactite than those at the other sites.

TABLE 2. DRIP SITE CHARACTERISTICS AND STABLE ISOTOPE COMPOSITIONS OF CALCITE AND WATER FROM HARRISON'S CAVE, BARBADOS

| | Site | | |
|---|---|---|---|
| | BC-98-1 | BC-98-2 | BC-98-3 |
| Maximum calcite thickness (mm) | 0.8 | 0.7 | 1.1 |
| Drip rate (mL/min) | 0.1–0.3 | 0.1–0.2 | 0.1–0.3 |
| Stalactite length (cm) | 25 | 40 | 7 |
| Cave air temp. (°C) 11 July 1998 | 26.3 | 26.3 | 26.3 |
| Cave air temp. (°C) 1 Feb. 1999 | 25.9 | 25.9 | 25.9 |
| $\delta^{13}C$ value (VPDB) | | | |
| DIC 9 July 1998 | –12.1 | –10.1 | NA |
| DIC 11 July 1998 | –11.5 | –9.8 | –10.9 |
| DIC 1 Feb. 1999 | –13.4 | –11.4 | –13.5 |
| DIC 1 July 2000 | –12.7 | –9.9 | –12.8 |
| Plate calcite minimum | –11.3 | –8.1 | –11.5 |
| Plate calcite maximum | –7.1 | –5.2 | –4.9 |
| Stalagmite tips | –10.1 | –8.0 | –10.5† |
| Minimum calcite in equil.* with DIC | –11.4 | –9.4 | –11.5 |
| Maximum calcite in equil.* with DIC | –9.5 | –7.8 | –8.9 |
| $\delta^{18}O$ value (SMOW) | | | |
| Drip water 9 July 1998 | –2.7 | –2.7 | NA |
| Drip water 1 Feb. 1999 | –2.7 | –2.8 | –2.7 |
| Drip water 1 July 2000 | –2.8 | –2.7 | –2.9 |
| $\delta^{18}O$ value (VPDB) | | | |
| Plate calcite minimum | –4.1 | –3.3 | –4.0 |
| Plate calcite maximum | –3.0 | –2.6 | –2.3 |
| Stalagmite tips | –3.8 | –3.3 | –3.9† |
| Minimum calcite in equil.* with drip | –5.3 | –5.3 | –5.3 |
| Maximum calcite in equil.* with drip | –5.4 | –5.4 | –5.5 |

*Note:* VPDB—Vienna Peedee belemnite; DIC—dissolved inorganic carbon; SMOW—standard mean ocean water.
*Isotopic equilibrium calculated at 26.1 °C.
†Average of two samples.

## METHODS

### Collection of Modern Calcite

Glass plate calcite was collected by placing 10 cm × 10 cm frosted glass plates on actively growing stalagmites. Glass plates were prepared by frosting with a sandblaster and then cleaning in an ultrasonic bath in microsolution, followed by de-ionized water. These stalagmites were first covered with a plastic bag to protect them from the experiment (Fig. 2). A modeling-clay base was constructed on the bag, and the plates were placed on the clay base so they were horizontal and the discrete drip feeding the speleothem fell in the middle of the plate. Glass plates were placed on 1 February 1999 and were collected on 1 July 2000. In addition, cores of the underlying stalagmite tips were collected (Mickler et al., 2004).

This glass plate method of evaluating speleothem isotopic equilibrium supports cave conservation, because collecting speleothem calcite on glass plates causes no permanent damage to cave formations. Because this method is nondestructive, a great many sites can be studied, increasing our understanding of the controls on the chemistry of speleothems potentially with much higher temporal resolution than is possible with natural cave formations. Alternatively, coring the tips of, or collecting whole, actively growing stalagmites and stalactites, or breaking the tips of soda straws, is required to obtain similar data. This glass plate method is effective for assessing isotopic equilibrium during calcite precipitation on the basis of the similarity of both carbon and oxygen isotope composition of the center of the glass plate calcite and the underlying stalagmite tips (Mickler et al., 2004).

### Plate Sampling

Temporal variability in the $\delta^{18}O$ and $\delta^{13}C$ values of plate calcite was assessed by sampling calcite, using a dental drill, from a 1 $cm^2$ area near the locus of precipitation on the glass plate (Fig. 3A). The calcite within this 1 $cm^2$ area was sampled in 0.02 mm layers over its entire thickness. This is analogous to sampling a speleothem along the growth axis. The relative heights of the dental drill and glass plates were monitored using a digital micrometer with a resolution of 1 μm.

The spatial variability in the oxygen and carbon isotope composition of the calcite was assessed by sampling calcite in a grid with a spacing of 2 cm × 2 cm (Fig. 3). At each grid point a small area ~2 mm in diameter was sampled, using a dental drill, encompassing the entire thickness of the calcite. This is analogous to sampling a speleothem along an individual growth layer.

### Carbon and Oxygen Isotopic Composition of Calcite

Calcite samples were analyzed for carbon and oxygen isotope composition at the University of Texas at Austin. Approximately 200–350 μg of calcite was analyzed in individual reaction vessels at 90 °C, using a Micromass Multiprep system. The resulting gas was released into a VG Prism II dual-inlet, triple-collector mass spectrometer and analyzed using standard

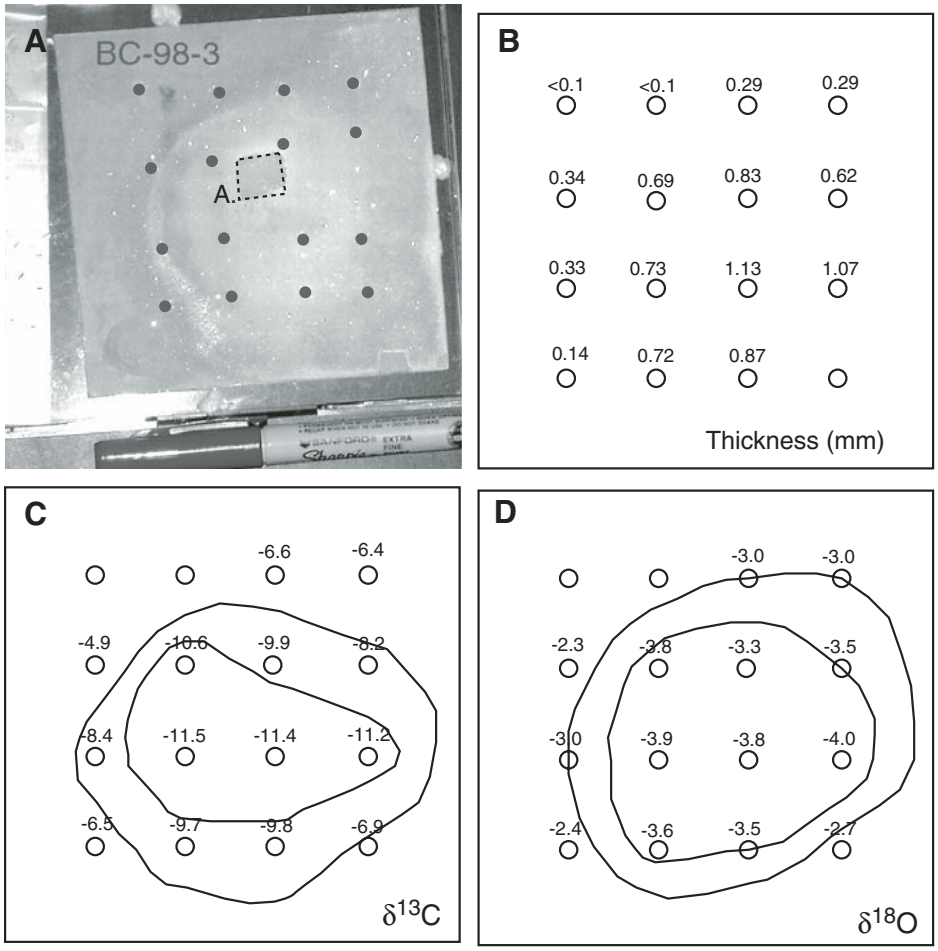


**Figure 3. Spatial variations at site BC-98-3. (A) Photograph of glass plate BC-98-3; ~1 cm² area was sampled to determine the temporal variability of calcite $\delta^{13}C$ and $\delta^{18}O$ values at A; small sample pits were drilled on a 2 cm × 2 cm grid to determine the spatial distribution of calcite $\delta^{13}C$ and $\delta^{18}O$ values. (B) Spatial distribution of calcite thickness. (C) Spatial distribution of $\delta^{13}C$ values of calcite, with –10‰ and –8‰ isopleths shown. (D) Spatial distribution of $\delta^{18}O$ values of calcite, with –3.5‰ and –3.0‰ isopleths shown.**

procedures. Analytical precision was 0.18‰ for $\delta^{18}O$ values and 0.12‰ for $\delta^{13}C$ values (2 σ of 40 standard runs). The results of isotopic analysis are presented in conventional delta (δ) notation, defined as $\delta = [(R_{sample} - R_{standard})/R_{standard}] \times 1000$, where $R$ is the ratio $^{18}O/^{16}O$ or $^{13}C/^{12}C$. The oxygen and carbon isotope values for carbonate samples and the carbon isotope values of DIC are expressed relative to the Vienna Peedee belemnite (VPDB) standard.

### Field Chemistry

Water was collected on three dates (11 July 1998, 1 February 1999, 1 July 2000) by placing a 1L polypropylene bottle on top of the stalagmites for 24 h, at which time water temperature and pH were measured, using a pH electrode and temperature probe. Two 40 mL amber VOA vials were collected for each water sample for alkalinity determination and $\delta^{13}C$ value of DIC. These samples were transported in a dark and cool container, and alkalinities were determined at the end of each field day by titrating 25 mL of cave water to a pH of 4.5, using 0.1M HCl.

### Carbon and Oxygen Isotopic Composition of Waters

Cave water samples were prepared for $\delta^{18}O$ analysis by equilibrating $CO_2$ with 300 µL of water at 40 °C for 7 h, using a Micromass Multiprep system, and analyzed on a VG Prism II dual-inlet mass spectrometer at the University of Texas at Austin. The oxygen isotopic values of water samples are expressed relative to Vienna Standard Mean Ocean Water. Analytical precision (2 σ) was 0.1‰, as determined by analysis of internal laboratory standards.

The C isotopic composition of dissolved inorganic carbon was determined by injecting 5 mL of the cave drip water into an evacuated sample vial with $H_3PO_4$. The resulting mixture of $CO_2$, water vapor, and noncondensable gases was released into a vacuum line, and the $CO_2$ was cryogenically purified. The $CO_2$ gas was analyzed on a VG Prism II dual inlet mass spectrometer. Analytical precision (2 σ of 0.1‰) was determined by analyzing a solution of $Na_2CO_3$ (aq) with a known C isotope composition and DIC concentrations similar to cave drip waters.

### Cation Analysis

Approximately 15 mL of cave water was collected in an acid-cleaned polypropylene bottle and acidified to 1‰, using ultrapure $HNO_3$, after it was returned to the University of Texas. Major elemental concentrations were analyzed from these waters at the University of Minnesota, using an inductively-coupled-plasma mass spectrometer, Perkin Elmer/Sciex Elan 5000 (Xia et al., 1997).

## RESULTS

Calcite grown on the glass plate was deposited much like a natural speleothem. The greatest calcite thickness was found where the cave drip fell on the plate, analogous to the component of maximum calcite growth along the speleothem growth axis (Fig. 3A and B). The calcite thickness decreased away from the growth axis from maximum thicknesses of 1.1 mm on plate BC-98-3 to a minimum value of <0.1 mm. Microscopy reveals rhombohedral crystals hundreds of micrometers in diameter, suggesting calcite mineralogy, which was confirmed by powder X-ray diffraction analysis.

The spatial variability in $\delta^{13}C$ and $\delta^{18}O$ values of glass plate calcite shows consistent trends. The $\delta^{13}C$ values of calcite from sites BC-98-1, BC-98-2, and BC-98-3 increase away from the growth axes (Fig. 3C). Only the lowest $\delta^{13}C$ values, those near the growth axes, are consistent with precipitation in C isotope equilibrium with DIC of the corresponding drip waters (Table 2; Fig. 4), as are the tips of the corresponding stalagmites (Mickler et al., 2004). Some $^{13}C$ enrichment likely occurs in the DIC due to $CO_2$ degassing during collection of the water samples, and possibly during storage prior to analysis. Adjusting the DIC $\delta^{13}C$ values for such an effect would only increase the extent of C isotope disequilibrium observed between DIC and the plate calcites.

The $\delta^{18}O$ values of calcite from the glass plates also increase progressively away from the growth axes (Fig. 3D). In all three plates the lowest $\delta^{18}O$ value of the calcite is higher than equilibrium values by 1.2‰ to 2.0‰, as are the tips of the corresponding stalagmites (Table 2). There is little temporal or spatial variation in the oxygen isotope composition of the drip waters and groundwaters throughout Barbados, nor is there substantial variation among the drip sites described here (Table 2; see also Jones et al., 2000; Jones and Banner, 2003). The mechanisms responsible for the high $\delta^{18}O$ values are outlined in Mickler et al. (2004). Briefly, the $\delta^{18}O$ values of calcite that exceed those in oxygen isotope equilibrium with coexisting water likely result from the combination of direct incorporation of $HCO_3^-$ into the calcite during rapid calcite precipitation, and the evolution of the $HCO_3^-$ reservoir during progressive calcite precipitation as modeled by Rayleigh distillation.

The $\delta^{13}C$ and $\delta^{18}O$ values of the spatially sampled calcite from the three plates exhibit a strong positive correlation, characterized by the orthogonal regression line $\delta^{13}C = 4.2 + 3.9 \times \delta^{18}O$ ($R^2 = 0.84$), with minimum $\delta^{13}C$ and $\delta^{18}O$ values of −11.5‰ and −4.1‰, and maximum $\delta^{13}C$ and $\delta^{18}O$ values of −4.9‰ and −2.3‰, respectively (Fig. 4). Site BC-98-3 shows the largest $^{13}C$ and $^{18}O$ enrichments away from the growth axis of 6.6‰ and 1.7‰, respectively.

Calcite sampled vertically, and thus temporally, along the growth axis shows a similar trend. The $\delta^{13}C$ versus $\delta^{18}O$ values of all three plates fall along the line $\delta^{13}C = 3.9 + 3.8 \times \delta^{18}O$ ($R^2 = 0.94$) (Fig. 5). Individual plates sampled along the growth axis exhibit low isotopic variability. Only plate BC-98-3 shows a significant positive covariance (line A, $\delta^{13}C = -2.7 + 2.1 \times \delta^{18}O$, $R^2 = 0.59$) between $\delta^{18}O$ and $\delta^{13}C$ values.

### Theoretical Determination of Potential Extent of DIC Loss

Calcite speleothem formation typically results when water, at or near equilibrium with a high $P_{CO_2}$ soil environment and calcite, enters the cave environment with a lower $P_{CO_2}$ (Holland et al., 1964). The water will move toward chemical equilibrium with its new environment by degassing $CO_2$, and the calcite precipitation-dissolution reaction (equation 1) will be driven to the right and calcite will precipitate.

$$2HCO_3^- + Ca^{++} \leftrightarrow CaCO_3 + CO_2 + H_2O. \quad (1)$$

As calcite precipitation, driven by $CO_2$ degassing, progresses, the $HCO_3^-$ reservoir in the drip water will undergo $^{13}C$ enrichment if C isotope exchange reactions between DIC and $CO_2$ (g) in

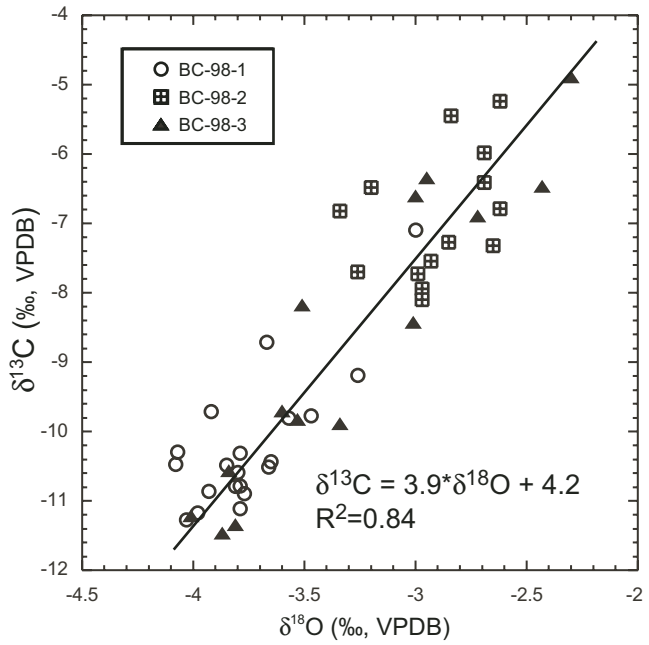


**Figure 4. $\delta^{13}C$ vs. $\delta^{18}O$ plot of glass plate calcite sampled spatially (as shown in Fig. 3) for plates from sites BC-98-1, BC-98-2, and BC-98-3. VPDB—Vienna Peedee belemnite.**

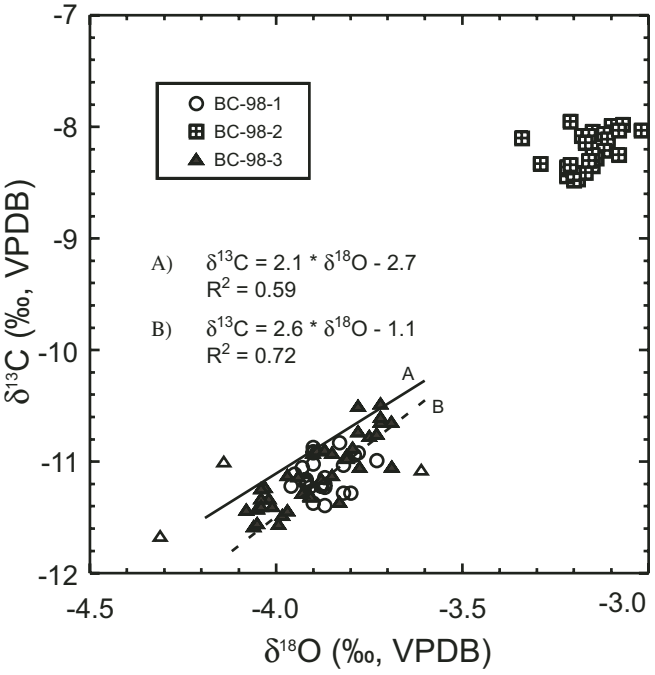


**Figure 5. $\delta^{13}C$ vs. $\delta^{18}O$ plot of glass plate calcite sampled along vertical transects near the locus of precipitation to determine the temporal variation of stable isotopes. On plates BC-98-1 and BC-98-2, there is not enough temporal variability to produce a significant trend in the data. Plate BC-98-3 does show a positive correlation between $\delta^{13}C$ and $\delta^{18}O$ values, indicated by line A. Excluding the samples with the two lowest and one highest $\delta^{18}O$ values (open triangles) yields a slope of 2.6 (dashed line B). A regression line through all the data can be expressed by the line $\delta^{13}C = 3.8 \times \delta^{18}O + 3.9$.**

the cave atmosphere are sufficiently slow. This $^{13}C$ enrichment results from the relatively low $\delta^{13}C$ value of the $CO_2$ that is lost from the drip water by degassing. The extent of $^{13}C$ enrichment is a function of the fractionation factors between the C species and the fraction of total DIC lost to $CO_2$ degassing and $CaCO_3$ precipitation. This isotopic evolution may be modeled as a Rayleigh distillation process, as discussed in Bar-Matthews et al. (1996) and Mickler et al. (2004). The fraction of DIC lost to degassing and calcite precipitation was estimated by modeling the evolution of the geochemical composition of the cave water, using the PHREEQC program (Parkhurst and Appelo, 1999). Several assumptions are made in the modeling: (1) Upon entry into the cave environment and prior to $CO_2$ degassing, the water is in chemical equilibrium with a high $P_{CO_2}$ soil environment and calcite (Table 3B). To calculate this end member, PHREEQC was used to model $CO_2$ addition to bring the collected water, which was supersaturated with calcite, to chemical equilibrium with calcite. (2) The geochemical composition of the water collected in the cave has been altered since first entering the cave by $CO_2$ degassing, but not $CaCO_3$ precipitation, prior to measuring alkalinity, pH, and DIC $\delta^{13}C$. The presence of the stalactites indicates some calcite precipitation prior to drip water sampling. Neglecting this process underestimates the amount of DIC initially present upon entry of the drip water into the cave. (3) $CO_2$ degassing and $CaCO_3$ precipitation (equation 1) continue until the water is in chemical equilibrium with cave $P_{CO_2}$ and calcite (Table 3C). Assumptions 1 and 3 define two end-member conditions of DIC concentrations that conservatively define the possible range of DIC loss. In this study, atmospheric $P_{CO_2}$ was used as the end member because cave $P_{CO_2}$ was not measured, but natural cave environments commonly have $P_{CO_2}$ concentrations higher than atmospheric values.

TABLE 3. HARRISON'S CAVE WATER CHEMISTRY

| Site | Date m/d/y | pH | Concentration (mol/L) | | | | | Fraction of DIC | | | SI |
|---|---|---|---|---|---|---|---|---|---|---|---|
| | | | $Ca^{+2}$ ($\times10^{-3}$) | DIC ($\times10^{-3}$) | $CO_2$* ($\times10^{-4}$) | $HCO_3^-$ ($\times10^{-3}$) | $CO_3^{-2}$ ($\times10^{-5}$) | $CO_2$* | $HCO_3^-$ | $CO_3^{-2}$ | |
| (A) Chemistry of water collected in the cave | | | | | | | | | | | |
| BC-98-1 | 2/1/99 | 7.8 | 2.18 | 4.41 | 1.29 | 4.14 | 1.72 | 0.03 | 0.94 | 0.00 | 0.76 |
| | 7/1/00 | 8.1 | 1.83 | 4.19 | 0.64 | 3.98 | 3.08 | 0.02 | 0.95 | 0.01 | 0.93 |
| BC-98-2 | 2/1/99 | 8.1 | 1.84 | 4.07 | 0.60 | 3.85 | 3.18 | 0.01 | 0.95 | 0.01 | 0.97 |
| | 7/1/00 | 8.1 | 1.49 | 3.01 | 0.49 | 2.87 | 2.08 | 0.02 | 0.95 | 0.01 | 0.71 |
| BC-98-3 | 2/1/99 | 7.7 | 2.14 | 4.36 | 1.59 | 4.08 | 1.35 | 0.04 | 0.93 | 0.00 | 0.66 |
| | 7/1/00 | 8.1 | 1.96 | 4.24 | 0.69 | 4.02 | 2.92 | 0.02 | 0.95 | 0.01 | 0.94 |
| (B) Calculated water chemistry in equilibrium with calcite and a theorized high $pCO_2$, as described in text | | | | | | | | | | | |
| BC-98-1 | 2/1/99 | 7.0 | 2.18 | 5.10 | 7.75 | 4.22 | 2.98 | 0.15 | 0.83 | 0.00 | |
| | 7/1/00 | 7.1 | 1.83 | 4.81 | 6.07 | 4.12 | 3.50 | 0.13 | 0.86 | 0.00 | |
| BC-98-2 | 2/1/99 | 7.1 | 1.84 | 4.72 | 6.24 | 4.01 | 3.32 | 0.13 | 0.85 | 0.00 | |
| | 7/1/00 | 7.4 | 1.49 | 3.27 | 2.65 | 2.95 | 4.06 | 0.08 | 0.90 | 0.00 | |
| BC-98-3 | 2/1/99 | 7.0 | 2.14 | 4.99 | 7.52 | 4.14 | 2.96 | 0.15 | 0.83 | 0.00 | |
| | 7/1/00 | 7.1 | 1.96 | 4.89 | 6.50 | 4.15 | 3.33 | 0.13 | 0.85 | 0.00 | |
| (C) Calculated water chemistry in equilibrium with calcite and atmospheric $CO_2$, allowing calcite precipitation to equilibrium, as described in text | | | | | | | | | | | |
| BC-98-1 | 2/1/99 | 8.3 | 4.53 | 0.87 | 8.31 | 0.84 | 1.02 | 0.01 | 0.96 | 0.01 | |
| | 7/1/00 | 8.4 | 3.03 | 1.14 | 8.98 | 1.10 | 1.58 | 0.01 | 0.97 | 0.01 | |
| BC-98-2 | 2/1/99 | 8.4 | 3.14 | 1.03 | 8.23 | 1.00 | 1.44 | 0.01 | 0.97 | 0.01 | |
| | 7/1/00 | 8.3 | 4.56 | 0.93 | 8.98 | 0.90 | 1.06 | 0.01 | 0.97 | 0.01 | |
| BC-98-3 | 2/1/99 | 8.2 | 4.87 | 0.94 | 10.39 | 0.91 | 0.95 | 0.01 | 0.97 | 0.01 | |
| | 7/1/00 | 8.4 | 3.64 | 1.04 | 8.98 | 1.00 | 1.31 | 0.01 | 0.97 | 0.01 | |

| | | Fractional loss | | | Potential $^{13}C$ enrichment owing to DIC loss (‰) |
|---|---|---|---|---|---|
| | | DIC | $HCO_3^-$ | $Ca^{+2}$ | |
| (D) DIC losses based on water compositions | | | | | |
| BC-98-1 | 2/1/99 | 0.83 | 0.80 | 0.79 | 6.0 |
| | 7/1/00 | 0.76 | 0.73 | 0.83 | 4.8 |
| BC-98-2 | 2/1/99 | 0.78 | 0.75 | 0.83 | 5.1 |
| | 7/1/00 | 0.72 | 0.70 | 0.69 | 4.3 |
| BC-98-3 | 2/1/99 | 0.81 | 0.78 | 0.77 | 5.6 |
| | 7/1/00 | 0.79 | 0.76 | 0.81 | 5.3 |

*Note*: $Ca^{+2}$ error ± 0.05 × $10^{-3}$ mol/L; $CO_2$* = $CO_2$ (aq) + $H_2CO_3$ (aq). DIC—dissolved organic carbon.

## Maximum Modeled $^{13}C$ and $^{18}O$ Enrichment

An estimation of the maximum $^{13}C$ enrichment in the $HCO_3^-$ reservoir owing to $CO_2$ degassing and $CaCO_3$ precipitation was made, using a Rayleigh distillation model outlined in Bar-Matthews et al. (1996) and Mickler et al. (2004), published isotope fractionation factors, and the conservative upper limit estimation of DIC loss described in the previous section. The effects of Rayleigh distillation on the $\delta^{13}C$ value of the DIC reservoir can be modeled by:

$$(\delta + 1000)/(\delta_o + 1000) = f^{(\alpha_{p\text{-}r}-1)}, \qquad (2)$$

where $\delta$ is the C isotope composition of $HCO_3^-$ (aq), $\delta_o$ is the initial C isotope composition of $HCO_3^-$ (aq), $f$ is the fraction of $HCO_3^-$ (aq) remaining at a given point in the drip water's evolution, and $\alpha_{p\text{-}r}$ is the equilibrium carbon isotope fractionation factor between a bulk product and the $HCO_3^-$ (aq) reactant. The variable $f$ was estimated by using the extent of DIC loss with the results given in Table 3 and discussed in the previous section. Because the C in $HCO_3^-$ (aq) is evenly partitioned between $CaCO_3$ and $CO_2$ (g) during calcite precipitation, we define a fractionation factor between a bulk product and $HCO_3^-$ (aq) such that $\alpha_{(\text{bulk product} - HCO_3^-)}$ is $1/2(\alpha_{CO_2 - HCO_3^-}) + 1/2(\alpha_{\text{calcite} - HCO_3^-})$. Using fractionation factors for $\alpha_{CO_2 - HCO_3^-}$ and $\alpha_{\text{calcite} - HCO_3^-}$ of 0.9922 and 1.0010, respectively (Romanek et al., 1992; Zhang et al., 1995), the $\alpha_{(\text{bulk product} - HCO_3^-)}$ is 0.9966 at 26.1 °C, the average temperature measured at the glass plate sites during calcite collection (Table 2).

We modeled the oxygen isotope effects of $CO_2$ degassing, $CaCO_3$ precipitation, and $H_2O$ formation, using an analogous Rayleigh distillation approach with the following assumptions: There is no oxygen isotope exchange between DIC and water, and the fractionation factor between the bulk product and $HCO_3^-$ (reactant) is $2/6(\alpha_{CO_2 - HCO_3^-}) + 3/6(\alpha_{\text{calcite} - HCO_3^-}) + 1/6(\alpha_{H_2O - HCO_3^-})$, or in proportion to the oxygen in each of the three products. Using fractionation factors for $\alpha_{CO_2 - HCO_3^-}$, $\alpha_{\text{calcite} - HCO_3^-}$, and $\alpha_{H_2O - HCO_3^-}$ of 1.0062, 0.9939, and 0.9667, respectively, the $\alpha_{(\text{bulk product} - HCO_3^-)}$ is 0.9935 at 26.1 °C. Fractionation factors between $HCO_3^-$ and other O-bearing species in equation 1 were calculated from the fractionation factors of Brenninkmeijer et al. (1983), Usdowski and Hoefs (1993), and Kim and O'Neil (1997).

This approach is an end-member calculation because it neglects $CO_2$ hydration and hydroxylation reactions (equations 3 and 4), which will buffer the oxygen isotopic composition of the $HCO_3^-$ (aq) reservoir and reduce the magnitude of the oxygen isotope effects of $CO_2$ degassing.

The forward and backward reactions outlined in equations 3 and 4 will result in the $HCO_3^-$ acquiring a $\delta^{18}O$ value closer to equilibrium with the large reservoir of oxygen in $H_2O$. Note that in the pH range of interest, reaction 3 is dominant.

$CO_2$ hydration

$$CO_2 + H_2O \leftrightarrow H_2CO_3 \leftrightarrow HCO_3^- (aq) + H^+ \quad (3)$$

and

$CO_2$ hydroxylation

$$CO_2 + OH^- \leftrightarrow HCO_3^- (aq). \quad (4)$$

This model of progressive loss of $HCO_3^-$ during calcite precipitation (equation 1), while excluding oxygen isotope exchange between DIC and $H_2O$, will cause progressive $^{18}O$ and $^{13}C$ enrichment in the $HCO_3^-$ reservoir, as shown in Figure 1B.

We use Rayleigh distillation to model the C isotope evolution of precipitating calcite because if carbon isotopes are fractionated during calcite precipitation, there must be an effect on the isotope composition of the remaining reactant. During rapid mineral precipitation, like that of speleothem formation, it is not uncommon for isotopic disequilibrium to occur (Fantidis and Ehhalt, 1970; Hendy, 1971). However, we use equilibrium fractionation factors as a best first approximation because they are known, whereas any deviation from isotopic equilibrium is unknown. If sufficient carbon is lost from the DIC reservoir to cause the observed $^{13}C$ enrichment across the glass plates, then this consumption of the $HCO_3^-$ should also affect the oxygen isotope composition. Only the relatively slow hydration-dehydration reactions permit oxygen isotope exchange with water, so if the precipitation of calcite proceeds rapidly, there may be progressive $^{18}O$ enrichment in the $HCO_3^-$ and in the $CO_3^-$ that is ultimately incorporated into the calcite. We recognize that excess $CO_2$ degassing beyond that in equation 1 would cause an additional increase in the $\delta^{13}C$ value, which could also be modeled by Rayleigh distillation with equilibrium fractionation factors (e.g., Michaelis et al., 1985). This process, however, should cause a decrease in the oxygen isotope ratios, whereas we observe coincident increases in both $\delta^{13}C$ and $\delta^{18}O$ values. A $CO_2$ degassing mechanism that can cause simultaneous increases in both $\delta^{13}C$ and $\delta^{18}O$ values is the kinetic isotope effect of the back reaction of equation 3 (dehydration), which is coupled to degassing (Hendy, 1971).

### Estimation of Potential DIC Loss and $^{13}C$ Enrichment in $HCO_3^-$ Reservoir

Water collected at the drip sites was supersaturated with respect to calcite as calculated from pH, temperature, alkalinity, and cation concentrations (Table 3A). This suggests that degassing of $CO_2$ prior to analysis altered the chemistry of the cave drip water. A maximum estimate of the possible extent of DIC losses is given in Table 3D. These calculations suggest that between 72% and 83% of the DIC could have been lost to $CO_2$ degassing and $CaCO_3$ precipitation. Modeling the C isotope effects by Rayleigh distillation indicates that this loss of DIC would result in a $^{13}C$ enrichment of the $HCO_3^-$ reservoir of 4.3‰ to 6.0‰ (Fig. 1B). These are maximum estimates of the potential enrichments, from progression of equation 1, because the cave environment likely has a higher $P_{CO_2}$ than atmospheric values. The maximum observed $^{13}C$ enrichment within a plate was 6.6‰ (BC-98-3), which is between 1.0‰ and 1.3‰ higher than the modeled results for the site BC-98-3 drips (Table 3D).

## DISCUSSION

### Rayleigh Distillation Model

Most of the C available for speleothem formation is held in the $HCO_3^-$ reservoir, and no other large source of C exists to buffer the $\delta^{13}C$ value of calcite. As $CO_2$ degassing and $CaCO_3$ precipitation proceed, there will be a progressive increase in the $\delta^{13}C$ value of the $HCO_3^-$ reservoir and the corresponding precipitated calcite. If $CO_2$ hydration and hydroxylation reactions are sufficiently fast relative to the rate of calcite precipitation, maintaining oxygen isotopic equilibrium between $HCO_3^-$ and $H_2O$, there will be no change in the $\delta^{18}O$ value of calcite during progressive $CO_2$ degassing and $CaCO_3$ precipitation, the processes causing $^{13}C$ enrichment. On a $\delta^{13}C$ versus $\delta^{18}O$ plot, this will manifest itself as a trend with a vertical slope, $\Delta\delta^{13}C/\Delta\delta^{18}O = \infty$ (Fig. 6, line A). If no $CO_2$ hydration and hydroxylation reactions are operating to buffer the $\delta^{18}O$ value of the $HCO_3^-$ reservoir, an end-member condition that will not occur in natural systems, then the isotopic composition of the $HCO_3^-$ reservoir, and thus the calcite, will evolve along a line with a slope of 0.52 at 26.1 °C (Fig. 6, line B). The slope of 0.52 represents the $\Delta\delta^{13}C/\Delta\delta^{18}O$ enrichment ratio modeled earlier by Rayleigh distillation (Fig. 1B). Owing to the temperature effect on the fractionation factors, this slope will vary with temperature, but this is a minor effect relative to the non-equilibrium isotope effects. A $\delta^{13}C$ versus $\delta^{18}O$ trend with an intermediate slope, between ∞ and 0.52, indicates that $CO_2$ hydration and hydroxylation reactions are too slow to maintain oxygen isotope equilibrium, and yet not so slow that no oxygen isotope exchange occurs. A hypothetical example of a $\Delta\delta^{13}C/\Delta\delta^{18}O$ slope of an intermediate value is given in Figure 6, line C.

### Spatial Isotopic Variability

When considered individually, the three drip sites each appear to produce distinct calcite carbon and oxygen isotope compositions and variability (Fig. 4). For instance, site BC-98-3 contains the lowest and most variable $\delta^{18}O$ and $\delta^{13}C$ values. Site BC-98-2 contains the highest average isotopic compositions, with the lowest variability. Thus, even though the three stalagmites occupy an area of ~1 $m^2$ in the same cave environment, each drip has its own unique isotopic and chemical composition (Tables 2 and 3). If these were ancient speleothems, one might infer distinct paleoenvironmental conditions for each.

When considered as a single system, the $\delta^{18}O$ and $\delta^{13}C$ results from sites BC-98-1, 2, and 3 follow the same linear trends (Fig. 4), consistent with the model outlined in Figure 6. Calcite precipitation and $CO_2$ degassing may be proceeding too fast for $CO_2$ hydration-hydroxylation reactions to buffer the oxygen isotope system

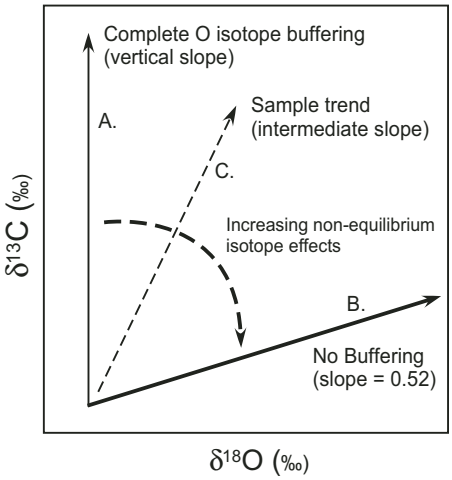


**Figure 6. Oxygen and carbon isotope effects of progressive loss of $HCO_3^-$ during $CO_2$ degassing and calcite precipitation on the $\delta^{18}O$ and $\delta^{13}C$ values of speleothem calcite. Line A: maintenance of oxygen isotopic equilibrium between dissolved inorganic carbon (DIC) through $CO_2$ hydration-hydroxylation reactions. Line B: absence of any oxygen isotopic exchange between dissolved inorganic carbon (DIC) and $H_2O$. Line C: intermediate path of isotope evolution in which incomplete oxygen isotopic buffering occurs.**

completely. This manifests itself by producing a positive correlation between $\delta^{18}O$ and $\delta^{13}C$ calcite values, in this case with a slope of 3.9. Because of this linear trend among the three drip sites, it is likely that upon entry into the cave environment, all three drips begin with similar DIC concentrations, DIC $\delta^{13}C$ values, and water $\delta^{18}O$ values.

Plate BC-98-3 exhibits the lowest isotopic composition and the highest isotopic variability; it also has the smallest stalactite feeding drip water to the plate site. Plate BC-98-2 exhibits the highest average isotopic values, and its drip flows over a much larger stalactite. Plate BC-98-1 has an intermediate isotopic composition and variability and is fed by an intermediate size stalactite. The correspondence of higher isotopic values with larger stalactites and higher isotopic variability with shorter stalactites may reflect progressive DIC loss by $CO_2$ degassing and calcite precipitation. The potential is greater for reaction progress along a longer stalactite prior to the drip water of a given composition depositing calcite on the stalagmite, or the glass plate. As a result, calcite precipitated on a stalagmite, or a glass plate, under a relatively shorter stalactite would be expected to have lower isotopic compositions and greater calcite thicknesses near the locus of precipitation, and greater isotopic variability along growth layers. By contrast, drip water of the same chemical composition, but which flows over a relatively larger stalactite, and subsequently has more time to degas $CO_2$ and precipitate calcite, would be expected to produce calcite with different growth and isotopic characteristics. All other factors being equal, calcite formed from water flowing over a relatively large stalactite would have higher isotopic compositions and lower calcite thicknesses near the locus of precipitation, and lower isotopic variability along growth layers.

Our experiment uses flat glass plates, which may affect the stable isotope composition of calcite along the growth layer by forcing the drip water to flow across a flat surface, unlike a natural convex stalagmite. This likely prolongs the residence time of drip water, relative to a natural stalagmite, allowing more time for $CO_2$ degassing and calcite precipitation. The range of $\delta^{18}O$ and $\delta^{13}C$ values of calcite precipitated near the locus of precipitation on the glass plates, however, is consistent with values obtained from the calcite along the growth axis of the plate's corresponding stalagmite tip (Mickler et al., 2004, Table 2). This suggests that the stable isotope composition of calcite along the growth axes is not affected by any increase in drip water residence times that may occur on the flat plates. The long drip water residence times on the glass plates relative to a convex natural stalagmite, along with our ability to sample very thin growth layers, may explain why we observe larger isotope variability along growth layers relative to natural stalagmites. Standard stalagmite sampling procedures, because of the difficulty of sampling discrete layers, may prevent the observation of the large isotopic variability seen on the glass plates.

The range of carbon isotope compositions observed on plates BC-98-1 and BC-98-2 can be explained by progressive loss of bicarbonate by the reaction represented by equation 1 and Figure 1B. However, only 5.3‰ to 5.6‰ of the 6.6‰ variation in the calcite $\delta^{13}C$ values observed on plate BC-98-3 can be accounted for by this modeled process. The ~1.0‰ carbon isotope enrichment on plate BC-98-3 in excess of that accounted for by the Rayleigh distillation model may be a consequence of other factors, including the following: (1) Rapid calcite crystallization may impart non-equilibrium carbon isotope fractionations between the calcite and the DIC. (2) $CO_2$ degassing simultaneously with calcite precipitation in excess of the 1:1 $CO_2$ to calcite stoichiometry of equation 1 would decrease the $\alpha_{(\text{bulk product} - HCO_3^-)}$, thereby causing a carbon isotope ratio increase in the remaining reactant bicarbonate. (3) Gaseous $^{13}C$ diffusional enrichment of up to 4.4‰ in the air boundary layer along the air-water interface might cause an increase in the $\delta^{13}C$ values if this $CO_2$ is incorporated back into the plate calcite. (4) The measured DIC chemistry of the drip waters collected at site BC-98-3 might be unrepresentative of the temporal variability at this site, and thus the potential reaction progress during calcite formation may be underestimated. Unfortunately, this study does not permit us to distinguish among these mechanisms.

## Temporal Isotopic Variability

Analysis of the $\delta^{13}C$ and $\delta^{18}O$ values of glass plate calcite sampled temporally in progressive layers near the locus of precipitation is analogous to sampling a speleothem along its growth axis. When plotted together, the $\delta^{13}C$ versus $\delta^{18}O$ values of the temporal samples fall on a line, $\delta^{13}C = 3.8 \times \delta^{18}O + 3.9$ (Fig. 5), with a similar slope and *y*-intercept to the regression line produced by glass plate calcite sampled spatially along the growth layer ($\delta^{13}C = 3.9 \times \delta^{18}O + 4.2$; Fig. 4). Individual drip sites show relatively little oxygen and carbon isotope variability, consistent with the limited isotopic variability in the waters. The site with the largest temporal variability, BC-98-3, exhibits a positive $\delta^{13}C$ versus $\delta^{18}O$ trend that may be controlled by the same mechanisms responsible for the isotopic variability seen along the growth layer.

Variation in the isotopic compositions along the growth axes of some ancient speleothems collected on Barbados, including several from Harrison's Cave, also show positive $\delta^{13}C$ versus $\delta^{18}O$ covariation, summarized in Table 1 (Mickler, 2004). These speleothems show a strong positive $\delta^{13}C$–$\delta^{18}O$ correlation of >99% confidence (3 of 8 samples), positive correlation of >95% confidence (1 of 8), and no significant correlation (4 of 8); see Table 1. Of the speleothems that exhibit no significant correlation, 1 of 4 (BN-3) has small stable isotope variability that makes it difficult to ascertain $\delta^{13}C$ versus $\delta^{18}O$ covariation. Two Holocene stalagmites from Barbados were collected from the Upper Passage of Harrison's Cave, the same room where modern glass plate calcite was collected. These stalagmites, BC-61 and BC-53, were similar in size to the stalagmites on which the glass plates were placed. BC-61 exhibits strong positive $\delta^{13}C$ versus $\delta^{18}O$ correlation with a slope of 2.7, similar to the temporal $\delta^{13}C$ versus $\delta^{18}O$ covariation seen in calcite from glass plate BC-98-3, whereas BC-53 has nonsignificant positive covariation. Each of these two stalagmites passes Hendy's (1971) layer tests for isotopic equilibrium on two of three layers studied, suggesting that these layer tests do not predict positive axial speleothem calcite carbon and oxygen isotopic covariation. Because several of these speleothems show strong positive $\delta^{13}C$ versus $\delta^{18}O$ covariation, the mechanism, or mechanisms, proposed to explain the temporal record must also explain the positive $\delta^{13}C$ versus $\delta^{18}O$ covariation.

## Implications for Speleothem-Based Climate Studies

Our results indicate that progressive $CO_2$ degassing and $CaCO_3$ precipitation may produce a positive covariance between $\delta^{13}C$ and $\delta^{18}O$ values, both along the speleothem growth layers and growth axes, with a slope >0.52. This covariation can be accounted for by Rayleigh distillation of the $HCO_3^-$ reservoir combined with incomplete oxygen isotopic equilibrium of the $HCO_3^-$ reservoir with $H_2O$. These non-equilibrium isotope effects may be influenced by climate. For example, increases in temperature will decrease $CO_2$ solubility and increase chemical reaction rates, including the oxygen isotope exchange rates between DIC and water (Mills and Urey, 1940), which may influence the kinetic isotope effects discussed in this paper. Conducting a similar plate study at a higher temporal resolution may document a climatic control on non-equilibrium isotope effects. Such research may help to calibrate isotopic shifts observed along speleothem growth

axes and growth layers to physical conditions in a cave environment, such as temperature, drip rates, calcite precipitation rates, stalactite geometry, and cave ventilation.

The positive correlation between $\delta^{13}C$ and $\delta^{18}O$ values of speleothem calcite sampled along the growth axis is commonly explained by climate change, discussed in detail in the section on Tests for Isotopic Equilibrium Precipitation of Stalagmite Calcite. The results of this study offer an additional explanation for positive $\delta^{13}C$ versus $\delta^{18}O$ covariation in speleothem calcite, and provide support for the tests for isotopic equilibrium calcite precipitation (Hendy, 1971; Desmarchelier et al., 2000).

A simultaneous increase in $\delta^{13}C$ and $\delta^{18}O$ values of speleothem calcite has been identified by other researchers who suggested that $CO_2$ degassing was responsible for $^{13}C$ enrichments but evaporation of the drip water was responsible for $^{18}O$ enrichments (Fornaca-Rinaldi et al., 1968; González and Lohmann, 1988). In our study, evaporative $^{18}O$ enrichment of cave water was discounted as a method of producing the observed 1.7‰ $^{18}O$ enrichments seen across the glass plate calcite at site BC-98-3 because of (1) the high relative humidity in the cave system (>98%), (2) the short residence time of the cave water on the glass plates (~30 min), and (3) the relatively large fraction of water that would have to be evaporated to produce the $^{18}O$ enrichments recorded in calcite sampled from the center to the edge of the glass plate (16%–19%).

TABLE 4. SUMMARY OF PUBLISHED SPELEOTHEM CARBON AND OXYGEN ISOTOPE RECORDS

| Category | Statistical descriptor† | Number | Percent | |
|---|---|---|---|---|
| (A) All stalagmites | | | | |
| - - | >99% confidence | 5 | 3.9 | Negative correlation |
| - | <95% confidence | 2 | 1.6 | |
| -,X | | 6 | 4.7 | No correlation |
| X | No correlation | 28 | 21.9 | 40.6% |
| +,X | | 5 | 3.9 | |
| + | <95% confidence | 11 | 8.6 | |
| + | | 22 | 17.2 | |
| + + | High confidence | 4 | 3.1 | Positive correlation |
| + + | >95% confidence | 3 | 2.3 | 55.5% |
| + + | >99% confidence | 42 | 32.8 | |
| | Total | 128 | | |
| (B) Quantitative stalagmite studies | | | | |
| - - | >99% confidence | 5 | 7.9 | Negative correlation |
| - | <95% confidence | 2 | 3.2 | No correlation |
| + | <95% confidence | 11 | 17.5 | 20.6% |
| + + | >95% confidence | 3 | 4.8 | Positive correlation |
| + + | >99% confidence | 42 | 66.7 | 71.4% |
| | Total | 63 | | |
| (C) Flowstones and stalactites | | | | |
| - | | 0 | 0.0 | Negative correlation |
| X | No correlation | 6 | 16.2 | No correlation |
| +,X | | 2 | 5.4 | 35.1% |
| + | <95% confidence | 5 | 13.5 | |
| + | | 10 | 27.0 | |
| + + | High confidence | 5 | 13.5 | Positive correlation |
| + + | >95% confidence | 2 | 5.4 | 64.9% |
| + + | >99% confidence | 7 | 18.9 | |
| | Total | 37 | | |

†Categories are as designated in Table 3.

### Prevalence of $\delta^{18}O$ and $\delta^{13}C$ Covariation in Speleothem Records

We reviewed published stable isotope studies of speleothems and found that many demonstrate carbon and oxygen isotope variations consistent with our proposed model (Table 1). These speleothem studies were broadly divided into three groups: those that show positive $\delta^{18}O$ and $\delta^{13}C$ covariation, those that show no covariation, and those that show negative $\delta^{18}O$ and $\delta^{13}C$ covariation (Table 4). Most stalagmites, 55% of 128 studies that presented both $\delta^{18}O$ and $\delta^{13}C$ values of stalagmite calcite sampled along growth axes, exhibit positive $\delta^{18}O$ versus $\delta^{13}C$ covariation. Some 41% of stalagmites show no correlation, and only 4% show negative $\delta^{18}O$ versus $\delta^{13}C$ correlation (Table 4A). The percentage of stalagmites that shows a significant or highly significant positive $\delta^{18}O$ versus $\delta^{13}C$ covariation increases to 71% of 63 studies when only studies that provide quantitative data are included (Table 4B). Most stable isotope studies of flowstones and stalactites also show positive $\delta^{18}O$ versus $\delta^{13}C$ covariations—65% of 37 studies (Table 4C). Even some speleothem records that show no apparent $\delta^{18}O$–$\delta^{13}C$ covariation for the entire data set contain shorter intervals that show strong positive covariations (Holmgren et al., 1999; Fig. 7B), and less commonly, strong negative covariations. Occasionally, some intervals are found that exhibit a vertical $\delta^{13}C$ versus $\delta^{18}O$ slope (e.g., Peqiin Cave; Bar-Matthews et al., 2003). Speleothem records in which the entire data set is negatively correlated also may contain short intervals that show strong positive $\delta^{13}C$ versus $\delta^{18}O$ covariations (Li et al., 1997, in Fig. 7 and Table 1). These short intervals that show positive $\delta^{13}C$ versus $\delta^{18}O$ covariation may be caused by variations in non-equilibrium isotope effects consistent with the model we propose to explain the isotopic variations in speleothems in Harrison's Cave.

Certainly not all positive $\delta^{18}O$ and $\delta^{13}C$ covariations in speleothem records shown in Table 1 are the result of kinetic isotope effects caused by $CO_2$ degassing and $CaCO_3$ precipitation that are independent of environmental conditions, as described in the Introduction. The Peqiin and Soreq Cave studies, e.g., show striking isotopic shifts that correspond to global climate changes, but they also manifest strong positive correlations in $\delta^{18}O$ and $\delta^{13}C$ values (Bar-Matthews et al., 2003). Even when strong positive $\delta^{18}O$–$\delta^{13}C$ covariations occur, possibly from non-equilibrium isotope effects, speleothem stable isotope records can still provide paleoclimatic information (e.g., Spötl and Mangini, 2002).

## IMPLICATIONS

Speleothem records may be influenced by kinetic isotope effects such that temperature-controlled equilibrium fractionation models alone cannot adequately explain the significance of the records. Proper interpretation of these records may require that the non-equilibrium isotope effects, causing $\delta^{13}C$ and $\delta^{18}O$ covariations in speleothems, be calibrated to physical conditions in the cave, such as temperature, cave $P_{CO_2}$, drip rates, calcite precipitation rates, stalactite geometry, and drip water chemistry.

#### ACKNOWLEDGMENTS

This work was supported by the Geology Foundation and the Environmental Science Institute of the University of Texas at Austin, the U.S. Department

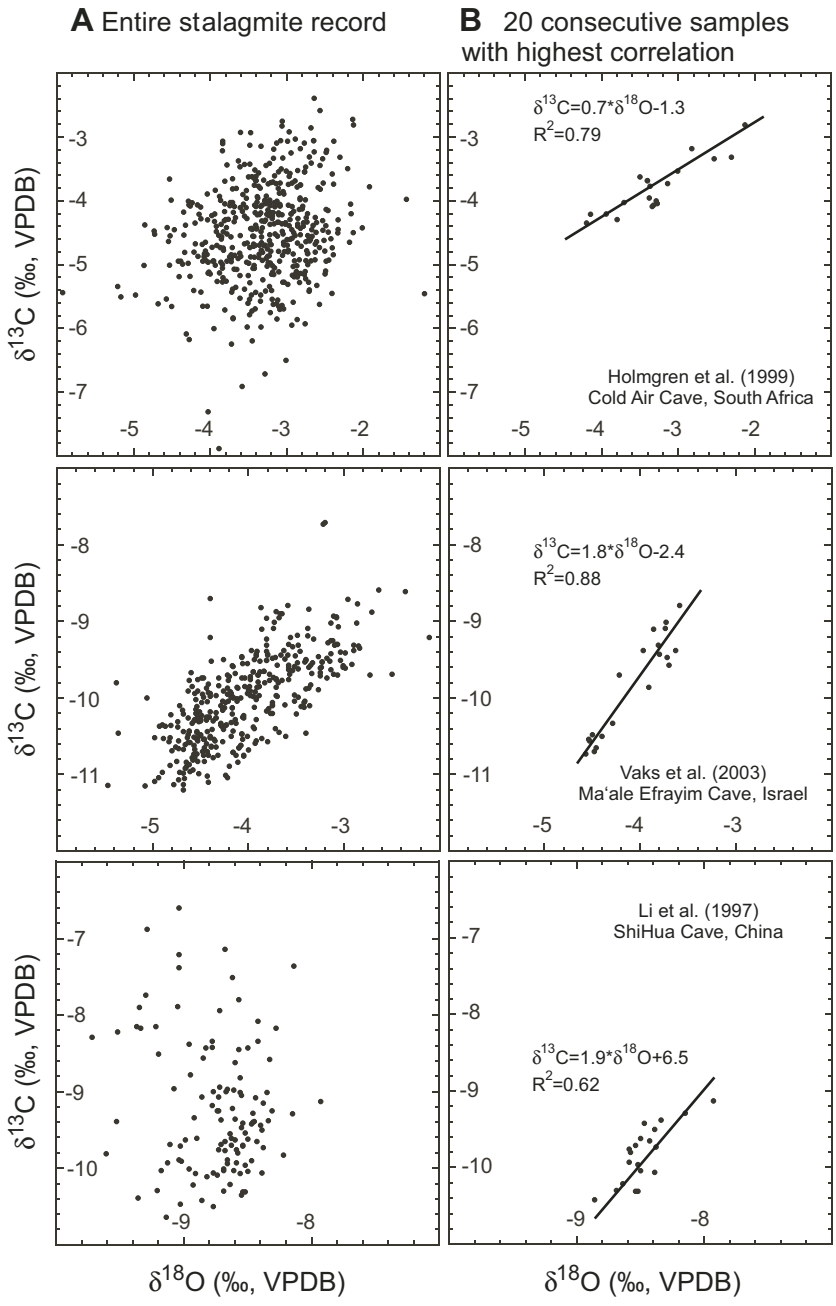


**Figure 7. $\delta^{13}C$ vs. $\delta^{18}O$ plots for three selected speleothem studies from the literature for which raw data were available. (A) Graphs of all the data. (B) Graphs of the 20 consecutive samples with the highest correlation coefficient. A subsample size of 20 was chosen because it provided a significant number of samples to determine correlation, and still maintained high temporal resolution. The slope and *y*-intercept produced by an orthogonal regression and correlation coefficients are shown.**

of Energy (DE-FG03-97ER14812), the U.S. National Science Foundation (EAR95-26714), and the Geological Society of America (7220-02). We appreciate the assistance provided by the management of Harrison's Cave, the Barbados National Trust, the Barbados Water Authority, the Bellairs Research Institute of McGill University, Tony Mason, Larry Mack, Emi Ito, and MaryLynn Musgrove.

## REFERENCES CITED

Allison, G.B., 1982, The relationship between $^{18}O$ and deuterium in water in sand columns undergoing evaporation: Journal of Hydrology, v. 55, p. 163–169, doi: 10.1016/0022-1694(82)90127-5.

Banner, J.L., Musgrove, M., Asmerom, Y., Edwards, R.L., and Hoff, J.A., 1996, High-resolution temporal record of Holocene ground-water chemistry; tracing links between climate and hydrology: Geology, v. 24, p. 1049–1053, doi: 10.1130/0091-7613(1996)024<1049:HRTROH>2.3.CO;2.

Bard, E., Delaygue, G., Rostek, F., Antonioli, F., Silenzi, S., and Schrag, D.P., 2002, Hydrological conditions over the western Mediterranean basin during the deposition of the cold sapropel 6 (ca. 175 kyr B.P.): Earth and Planetary Science Letters, v. 202, p. 481–494, doi: 10.1016/S0012-821X(02)00788-4.

Bar-Matthews, M., Ayalon, A., Matthews, A., Sass, E., and Halicz, L., 1996, Carbon and oxygen isotope study of the active water-carbonate system in a karstic Mediterranean cave: Implications for paleoclimate research in semiarid regions: Geochimica et Cosmochimica Acta, v. 60, p. 337–347, doi: 10.1016/0016-7037(95)00395-9.

Bar-Matthews, M., Ayalon, A., and Kaufman, A., 1997, Late Quaternary paleoclimate in the eastern Mediterranean region from stable isotope analysis of speleothems at Soreq Cave, Israel: Quaternary Research, v. 47, p. 155–168, doi: 10.1006/qres.1997.1883.

Bar-Matthews, M., Ayalon, A., Kaufman, A., and Wasserburg, G.J., 1999, The Eastern Mediterranean paleoclimate as a reflection of regional events: Soreq cave, Israel: Earth and Planetary Science Letters, v. 166, p. 85–95, doi: 10.1016/S0012-821X(98)00275-1.

Bar-Matthews, M., Ayalon, A., and Kaufman, A., 2000, Timing and hydrological conditions of Sapropel events in the Eastern Mediterranean, as evident from speleothems, Soreq cave, Israel: Chemical Geology, v. 169, p. 145–156, doi: 10.1016/S0009-2541(99)00232-6.

Bar-Matthews, M., Ayalon, A., Gilmour, M., Matthews, A., and Hawkesworth, C.J., 2003, Sea-land oxygen isotopic relationships from planktonic foraminifera and speleothems in the Eastern Mediterranean region and their implication for paleorainfall during interglacial intervals: Geochimica et Cosmochimica Acta, v. 67, p. 3181–3199, doi: 10.1016/S0016-7037(02)01031-1.

Baskaran, M., and Krishnamurthy, R.V., 1993, Speleothems as proxy for the carbon isotope composition of atmospheric $CO_2$: Geophysical Research Letters, v. 20, p. 2905–2908.

Berstad, I.M., Lundberg, J., Lauritzen, S.-E., and Linge, H.C., 2002, Comparison of the climate during marine isotope stage 9 and 11 inferred from a speleothem isotope record from Northern Norway: Quaternary Research, v. 58, p. 361–371, doi: 10.1006/qres.2002.2387.

Brenninkmeijer, C.A.M., Kraft, P., and Mook, W.G., 1983, Oxygen isotope fractionation between $CO_2$ and $H_2O$: Chemical Geology, Isotope Geoscience Section, v. 41, p. 181–190.

Burns, S.J., Fleitmann, D., Mudelsee, M., Neff, U., Matter, A., and Mangini, A., 2002, A 780-year annually resolved record of Indian Ocean monsoon precipitation from a speleothem from South Oman: Journal of Geophysical Research—Atmospheres, v. 107, p. 4434, doi: 10.1029/2001JD001281.

Cruz, F.W., Burns, S.J., Karmann, I., Sharp, W.D., Vuille, M., Cardoso, A.O., Ferrari, J.A., Dias, P.L.S., and Viana, O., 2005, Insolation-driven changes in atmospheric circulation over the past 116,000 years in subtropical Brazil: Nature, v. 434, p. 63–66, doi: 10.1038/nature03365.

Dansgaard, W., 1964, Stable isotopes in precipitation: Tellus, v. 16, p. 436–468.

De Geest, P., Verheyden, S., Cheng, H., Edwards, L., and Keppens, E., 2005, High-resolution speleothem records from Soqotra Island, Yemen: An approach to reconstruct Indian Ocean monsoon variability?: Geophysical Research Abstracts, v. 7, p. 03783.

Denniston, R.F., González, L.A., Asmerom, Y., Baker, R.G., Reagan, M.K., and Bettis, E.A., III, 1999a, Evidence for increased cool season moisture during the middle Holocene: Geology, v. 27, p. 815–818, doi: 10.1130/0091-7613(1999)027<0815:EFICSM>2.3.CO;2.

Denniston, R.F., González, L.A., Baker, R.G., Asmerom, Y., Reagan, M.K., Edwards, R.L., and Alexander, E.C., 1999b, Speleothem evidence for Holocene fluctuation of the prairie-forest ecotone, north-central USA: The Holocene, v. 9, p. 671–676, doi: 10.1191/095968399674716399.

Denniston, R.F., González, L.A., Semken, H.A., Jr., Asmerom, Y., Baker, R.G., Recelli-Snyder, H., Reagan, M.K., and Bettis, E.A., III, 1999c, Integrat-

ing stalagmite, vertebrate, and pollen sequences to investigate Holocene vegetation and climate change in the southern Midwestern United States: Quaternary Research, v. 52, p. 381–387, doi: 10.1006/qres.1999.2075.

Denniston, R.F., González, L.A., Asmerom, Y., Polyak, V., Reagan, M.K., and Saltzman, M.R., 2001, A high-resolution speleothem record of climatic variability at the Allerød–Younger Dryas transition in Missouri, central United States: Palaeogeography, Palaeoclimatology, Palaeoecology, v. 176, p. 147–155, doi: 10.1016/S0031-0182(01)00334-0.

Desmarchelier, J.M., and Goede, A., 1996, High resolution stable isotope analysis of a Tasmanian speleothem: Papers and Proceedings of the Royal Society of Tasmania, v. 130, p. 7–13.

Desmarchelier, J.M., Goede, A., Ayliffe, L.K., McCulloch, M.T., and Moriarty, K., 2000, Stable isotope record and its palaeoenvironmental interpretation for a late Middle Pleistocene speleothem from Victoria Fossil Cave, Naracoorte, South Australia: Quaternary Science Reviews, v. 19, p. 763–774, doi: 10.1016/S0277-3791(99)00037-2.

Dorale, J.A., Edwards, R.L., Ito, E., and González, L.A., 1998, Climate and vegetation history of the mid-continent from 75 to 25 ka: A speleothem record from Crevice Cave, Missouri, USA: Science, v. 282, p. 1871–1874, doi: 10.1126/science.282.5395.1871.

Dorale, J.A., Edwards, R.L., and Onac, B.P., 2002, Stable isotopes as environmental indicators in speleothems, *in* Yuan, D., and Zhang, C., eds., Karst processes and the carbon cycle, final report of IGCP379: Beijing, Geological Publishing House, p. 107–120.

Drysdale, R.N., Zanchetta, G., Hellstrom, J.C., Fallick, A.E., Zhao, J.-x., Isola, I., and Bruschi, G., 2004, Palaeoclimatic implications of the growth history and stable isotope ($\delta^{18}O$ and $\delta^{13}C$) geochemistry of a Middle to Late Pleistocene stalagmite from central-western Italy: Earth and Planetary Science Letters, v. 227, p. 215–229, doi: 10.1016/j.epsl.2004.09.010.

Duplessy, J.C., Lalou, C., de Azevedo, G., and Expedito, A., 1969, Etude des conditions de concretionnement dans les grottes au moyen des isotopes stables de l'oxygène et du carbone: Comptes Rendus des Séances de l'Académie des Sciences, sér. D, Sciences Naturelles, v. 268, p. 2327–2330.

Duplessy, J.C., Labeyrie, J., Lalou, C., and Nuygen, H.V., 1971, La mesure des variations climatiques continentales application à la période comprise entre 130,000 et 90,000 ans B.P.: Quaternary Research, v. 1, p. 162–174, doi: 10.1016/0033-5894(71)90039-1.

Edwards, R.L., Chen, J.H., and Wasserburg, G.J., 1987, $^{238}U$- $^{234}U$- $^{230}Th$- $^{232}Th$ systematics and the precise measurement of time over the past 500,000 years: Earth and Planetary Science Letters, v. 81, p. 175–192, doi: 10.1016/0012-821X(87)90154-3.

Fantidis, J., and Ehhalt, D.H., 1970, Variations of the carbon and oxygen isotopic composition in stalagmites and stalactites; evidence of non-equilibrium isotopic fractionation: Earth and Planetary Science Letters, v. 10, p. 136–144, doi: 10.1016/0012-821X(70)90075-0.

Farquhar, G.D., Ehleringer, J.R., and Hubick, K.T., 1989, Carbon isotope discrimination and photosynthesis: Annual Review of Plant Physiology and Plant Molecular Biology, v. 40, p. 503–537, doi: 10.1146/annurev.pp.40.060189.002443.

Fischer, M.J., Gale, S.J., Heijnis, H., and Drysdale, R.N., 1996, Low latitude speleothems and palaeoclimatic reconstruction: Karst Waters Institute Special Publication, v. 2, p. 26–29.

Fornaca-Rinaldi, G., Panichi, C., and Tongiorgi, E., 1968, Some causes of the variation in the isotopic composition of carbon and oxygen in cave concretions: Earth and Planetary Science Letters, v. 4, p. 321–324, doi: 10.1016/0012-821X(68)90095-2.

Frumkin, A., Carmi, I., Gopher, A., Ford, D.C., Schwarcz, H.P., and Tsuk, T., 1999, A Holocene millennial-scale climatic cycle from a speleothem in Nahal Qanah Cave, Israel: The Holocene, v. 9, p. 677–682, doi: 10.1191/095968399669422210.

Frumkin, A., Ford, D.C., and Schwarcz, H.P., 2000, Paleoclimate and vegetation of the last glacial cycles in Jerusalem from a speleothem record: Global Biogeochemical Cycles, v. 14, p. 863–870, doi: 10.1029/1999GB001245.

Gascoyne, M., 1992, Palaeoclimate determination from cave calcite deposits: Quaternary Science Reviews, v. 11, p. 609–632, doi: 10.1016/0277-3791(92)90074-I.

Gascoyne, M., Ford, D.C., and Schwarcz, H.P., 1981, Late Pleistocene chronology and paleoclimate of Vancouver Island determined from cave deposits: Canadian Journal of Earth Sciences, v. 18, p. 1643–1652.

Genty, D., Vokal, B., Obelic, B., and Massault, M., 1998, Bomb $^{14}C$ time history recorded in two modern stalagmites; importance for soil organic matter dynamics and bomb $^{14}C$ distribution over continents: Earth and Planetary Science Letters, v. 160, p. 795–809, doi: 10.1016/S0012-821X(98)00128-9.

Genty, D., Blamart, D., Ouahdi, R., Gilmour, M., Baker, A., Jouzel, J., and van Exter, S., 2003, Precise dating of Dansgaard-Oeschger climate oscillations in western Europe from stalagmite data: Nature, v. 421, p. 833–837, doi: 10.1038/nature01391.

Gewelt, M., 1981, Les variations isotopiques du carbone et de l'oxygène dans une stalagmite de la grotte de Remouchamps (Belgique): Méthodes et premiers résultats: Annales de la Société Géologique de Belgique, v. 104, p. 269–279.

Goede, A., 1994, Continuous early last glacial palaeoenvironmental record from a Tasmanian speleothem based on stable isotope and minor element variations: Quaternary Science Reviews, v. 13, p. 283–291, doi: 10.1016/0277-3791(94)90031-0.

Goede, A., and Vogel, J.C., 1991, Trace element variations and dating of a Late Pleistocene Tasmanian speleothem: Palaeogeography, Palaeoclimatology, Palaeoecology, v. 88, p. 121–131, doi: 10.1016/0031-0182(91)90018-M.

Goede, A., Green, D.C., and Harmon, R.S., 1986, Late Pleistocene palaeotemperature record from a Tasmanian speleothem: Australian Journal of Earth Sciences, v. 33, p. 333–342.

Goede, A., Veeh, H.H., and Ayliffe, L.K., 1990, Late Quaternary palaeotemperature records for two Tasmanian speleothems: Australian Journal of Earth Sciences, v. 37, p. 267–278.

Goede, A., McDermott, F., Hawkesworth, C., Webb, J., and Finlayson, B., 1996, Evidence of Younger Dryas and Neoglacial cooling in a late Quaternary palaeotemperature record from a speleothem in eastern Victoria, Australia: Journal of Quaternary Science, v. 11, p. 1–7, doi: 10.1002/(SICI)1099-1417(199601/02)11:1<1::AID-JQS219>3.3.CO;2-U.

González, L.A., and Gomez, R., 2002, High-resolution speleothem paleoclimatology of northern Venezuela: A progress report: Boletín Sociedad Venezolana de Espeleología, v. 36, p. 27–29.

González, L.A., and Lohmann, K.C, 1988, Controls on mineralogy and composition of spelean carbonates; Carlsbad Caverns, New Mexico, *in* James, N.P., and Choquette, P.W., eds., Paleokarst: New York, Springer-Verlag, p. 81–101.

Harmon, R.S., Schwarcz, H.P., and Ford, D.C., 1978a, Stable isotope geochemistry of speleothems and cave waters from the Flint Ridge–Mammoth Cave system, Kentucky: Implications for terrestrial climate change during the period 230,000 to 100,000 years B.P.: Journal of Geology, v. 86, p. 373–384.

Harmon, R.S., Thompson, P., Schwartz, H.P., and Ford, D.C., 1978b, Late Pleistocene paleoclimates of North America as inferred from stable isotope studies of speleothems: Quaternary Research, v. 9, p. 54–70, doi: 10.1016/0033-5894(78)90082-0.

Hellstrom, J., McCulloch, M.T., and Stone, J., 1998, A detailed 31,000-year record of climate and vegetation change, from the isotope geochemistry of two New Zealand speleothems: Quaternary Research, v. 50, p. 167–178, doi: 10.1006/qres.1998.1991.

Hendy, C.H., 1971, The isotopic geochemistry of speleothems—I. The calculation of the effects of different modes of formation on the isotopic composition of speleothems and their applicability as palaeoclimatic indicators: Geochimica et Cosmochimica Acta, v. 35, p. 801–824, doi: 10.1016/0016-7037(71)90127-X.

Hendy, C.H., and Wilson, A.T., 1968, Palaeoclimatic data from speleothems: Nature, v. 219, p. 48–51.

Holland, H.D., Kirsipu, T.W., Huebner, J.S., and Ocurgh, U.M., 1964, On some aspects of the chemical evolution of cave waters: Journal of Geology, v. 72, p. 36–67.

Holmgren, K., Karlén, W., and Shaw, P.A., 1995, Paleoclimatic significance of the stable isotopic composition and petrology of a late Pleistocene stalagmite from Botswana: Quaternary Research, v. 43, p. 320–328, doi: 10.1006/qres.1995.1038.

Holmgren, K., Karlén, W., Lauritzen, S.E., Lee-Thorp, J.A., Partridge, T.C., Piketh, S., Repinski, P., Stevenson, C., Svanered, O., and Tyson, P.D., 1999, A 3000-year high-resolution stalagmite-based record of palaeoclimate for northeastern South Africa: The Holocene, v. 9, p. 295–309, doi: 10.1191/095968399672625464.

Holmgren, K., Lee-Thorp, J.A., Cooper, G.R.J., Lundblad, K., Partridge, T.C., Scott, L., Sithaldeen, R., Talma, A.S., and Tyson, P.D., 2003, Persistent millennial-scale climatic variability over the past 25,000 years in Southern Africa: Quaternary Science Reviews, v. 22, p. 2311–2326.

Horvatinčić, N., Bronić, I.K., and Obelić, B., 2003, Differences in the $^{14}C$ age, $\delta^{13}C$ and $\delta^{18}O$ of Holocene tufa and speleothem in the Dinaric Karst: Palaeogeography, Palaeoclimatology, Palaeoecology, v. 193, p. 139–157, doi: 10.1016/S0031-0182(03)00224-4.

Hou, J.Z., Tan, M., Cheng, H., and Liu, T.S., 2003, Stable isotope records of plant cover change and monsoon variation in the past 2200 years: Evidence from laminated stalagmites in Beijing, China: Boreas, v. 32, p. 304–313, doi: 10.1080/03009480310002000.

Huang, J., 1992, The isotopic characteristics of carbon and oxygen of the Quaternary stalagmite in Shiquan Cave, Hubei, and paleoclimatic study: Carsologica Sinica, v. 11, p. 245–249.

Huang, J., Hu, C., Zhou, Q., and Lin, X., 2001, Stable isotope and trace element record of a stalagmite in Heshang Cave, Hubei and its palaeoclimatic significance: Science in China, ser. E, v. 44, p. 123–128.

Jiménez de Cisneros, C., Caballero, E., Vera, J.A., Durán, J.J., and Juliá, R., 2003, A record of Pleistocene climate from a stalactite, Nerja Cave, southern Spain: Palaeogeography, Palaeoclimatology, Palaeoecology, v. 189, p. 1–10, doi: 10.1016/S0031-0182(02)00589-8.

Jones, I.C., and Banner, J.L., 2003, Estimating recharge thresholds in tropical karst island aquifers: Barbados, Puerto Rico and Guam: Journal of Hydrology, v. 278, p. 131–143, doi: 10.1016/S0022-1694(03)00138-0.

Jones, I.C., Banner, J.L., and Humphrey, J.D., 2000, Estimating recharge in a tropical karst aquifer: Water Resources Research, v. 36, p. 1289–1299, doi: 10.1029/1999WR900358.

Kacanski, A., Carmi, I., Shemesh, A., Kronfeld, J., Yam, R., and Flexer, A., 2001, Late Holocene climatic change in the Balkans; speleothem isotopic data from Serbia: Radiocarbon, v. 43, p. 647–658.

Kadlec, J., Hladikova, J., and Zak, K., 1996, Isotopic study of cave carbonates from Moravian Karst, Czech Republic: Karst Waters Institute Special Publication, v. 2, p. 67–71.

Karst-Dynamics-Laboratory, Paleo-climate records from stalagmites in South China: http://www.karst.edu.cn/paleo/paleo.htm.

Kim, S.-T., and O'Neil, J.R., 1997, Equilibrium and nonequilibrium oxygen isotope effects in synthetic carbonates: Geochimica et Cosmochimica Acta, v. 61, p. 3461–3475, doi: 10.1016/S0016-7037(97)00169-5.

Labonne, M., Hillaire-Marcel, C., Ghaleb, B., and Goy, J.-L., 2002, Multi-isotopic age assessment of dirty speleothem calcite; an example from Altamira Cave, Spain: Quaternary Science Reviews, v. 21, p. 1099–1110, doi: 10.1016/S0277-3791(01)00076-2.

Lachniet, M.S., Asmerom, Y., Burns, S., Patterson, W.P., Polyak, V.J., and Seltzer, G.O., 2004a, Tropical response to the 8200 yr cold event? Speleothem isotopes indicate a weakened early Holocene monsoon in Costa Rica: Geology, v. 32, p. 957–960, doi: 10.1130/G20797.1.

Lachniet, M.S., Burns, S.J., Piperno, D.R., Asmerom, Y., Polyak, V.J., Moy, C.M., and Christenson, K., 2004b, A 1500-year El Niño/Southern Oscillation and rainfall history for the Isthmus of Panama from speleothem calcite: Journal of Geophysical Research—Atmospheres, v. 109, D20117, doi: 10.1029/2004JD004694.

Lauriol, B., Ford, D.C., Cinq-Mars, J., and Morris, W.A., 1997, The chronology of speleothem deposition in northern Yukon and its relationships to permafrost: Canadian Journal of Earth Sciences, v. 34, p. 902–911.

Lauritzen, S.-E., 1995, High-resolution paleotemperature proxy record for the last interglaciation based on Norwegian speleothems: Quaternary Research, v. 43, p. 133–146, doi: 10.1006/qres.1995.1015.

Lauritzen, S.-E., and Lundberg, J., 1999, Calibration of the speleothem delta function: An absolute temperature record for the Holocene in northern Norway: The Holocene, v. 9, p. 659–669, doi: 10.1191/095968399667823929.

Lauritzen, S.-E., and Lundberg, J., 2004, Isotope Stage 11, the "Super-Interglacial", from a north Norwegian speleothem, *in* Sasowsky, I.D., and Mylroie, J., eds., Studies of cave sediments: New York, Kluwer Academic, p. 257–272.

Lauritzen, S.-E., and Onac, B.P., 1999, Isotopic stratigraphy of a last interglacial stalagmite from northwestern Romania: Correlation with the deep-sea record and northern-latitude speleothem: Journal of Cave and Karst Studies, v. 61, p. 22–30.

Li, B., Yuan, D., Lauritzen, S.-E., Qin, J., and Lin, Y., 1998a, The Younger Dryas event and Holocene climate fluctuations recorded in a stalagmite from the Panlong Cave of Guilin: Acta Geologica Sinica—English Edition, v. 72, p. 455–465.

Li, B., Yuan, D., Qin, J., Lin, Y., and Zhang, M., 2000a, Oxygen and carbon isotopic characteristics of rainwater, drip water and present speleothems in a cave in Guilin area, and their environmental meanings: Science in China, ser. D, v. 43, p. 277–285.

Li, B., Yuan, D., Qin, J., and Zhang, M., 2000b, The paleoclimatic changes of Guilin area since 40,000 a B.P. and its dynamical mechanism: Acta Geoscientia Sinica, v. 21, p. 313–319, doi: 10.1007/s101140050024.

Li, H., Ku, T.-L., Chen, W., and Liu, T., 1997, Isotope studies of Shihua Cave—III: Reconstruction and paleoenvironment of Beijing during the last 3000 years from $\delta^{18}O$ and $\delta^{13}C$ records in stalagmite: Seismology and Geology, v. 19, p. 77–86.

Li, H., Gu, D., Stott, L.D., and Chen, W., 1998b, Applications of interannual-resolution stable isotope records of speleothem: Climatic changes in Beijing and Tianjin, China during the past 500 years; the $\delta^{18}O$ record: Science in China, ser. D, v. 41, p. 362–368.

Li, P., Peng, Z., Wen, Q., Li, Y., Yang, H., Hong, A., Xu, Z., Wang, M., He, J., Diao, S., and Ye, Y., 1996, Study on the stalagmite age and the paleotemperature of the Tian'e Cave in Ninghua, Fujian, China: Acta Sedimentologica Sinica, v. 14, p. 149–155.

Linge, H., Lauritzen, S.-E., and Lundberg, J., 2001a, Stable isotope stratigraphy of a late last interglacial speleothem from Rana, northern Norway: Quaternary Research, v. 56, p. 155–164, doi: 10.1006/qres.2001.2254.

Linge, H., Lauritzen, S.-E., Lundberg, J., and Berstad, I.M., 2001b, Stable isotope stratigraphy of Holocene speleothems; examples from a cave system in Rana, Northern Norway: Palaeogeography, Palaeoclimatology, Palaeoecology, v. 167, p. 209–224, doi: 10.1016/S0031-0182(00)00225-X.

Ma, Z., Li, H., Xia, M., Ku, T., Peng, Z., Chen, Y., and Zhang, Z., 2003, Paleotemperature changes over the past 3000 years in eastern Beijing, China: A reconstruction based on Mg/Sr records in a stalagmite: Chinese Science Bulletin, v. 48, p. 395–400, doi: 10.1360/03tb9083.

McDermott, F., 2004, Palaeo-climate reconstruction from stable isotope variations in speleothems: A review: Quaternary Science Reviews, v. 23, p. 901–918, doi: 10.1016/j.quascirev.2003.06.021.

McDermott, F., Frisia, S., Huang, Y., Longinelli, A., Spiro, B., Heaton, T.H.E., Hawkesworth, C.J., Borsato, A., Keppens, E., Fairchild, I.J., van der Borg, K., Verheyden, S., and Selmo, E., 1999, Holocene climate variability in Europe: Evidence from $\delta^{18}O$, textural and extension-rate variations in three speleothems: Quaternary Science Reviews, v. 18, p. 1021–1038, doi: 10.1016/S0277-3791(98)00107-3.

McDonald, J., Drysdale, R., Heijnis, H., and Ihlenfeld, C., 2001, Stable isotope and trace element geochemistry of speleothems from Cliefden Caves, central NSW: Implications for palaeoclimate reconstruction, Australasian Quaternary Association (AQUA) biennial conference: Port Fairy, Victoria, Australia, http://www.aqua.org.au/AQUA/aqua_2001.html.

Michaelis, J., Usdowski, E., and Menschel, G., 1985, Partitioning of $^{13}C$ and $^{12}C$ on the degassing of $CO_2$ and the precipitation of calcite—Rayleigh-type fractionation and a kinetic model: American Journal of Science, v. 285, p. 318–327.

Mickler, P.J., 2004, Controls on the stable isotopic composition of speleothems, Barbados, West Indies [Ph.D. thesis]: Austin, University of Texas, 160 p.

Mickler, P.J., Banner, J.L., Stern, L., Asmerom, Y., Edwards, R.L., and Ito, E., 2004, Stable isotope variations in modern tropical speleothems: Evaluating applications to paleoenvironmental reconstructions: Geochimica et Cosmochimica Acta, v. 68, p. 4381–4393, doi: 10.1016/j.gca.2004.02.012.

Mills, G.A., and Urey, H.C., 1940, The kinetics of isotopic exchange between carbon dioxide, bicarbonate ion, carbonate ion, and water: Journal of the American Chemical Society, v. 62, p. 1019–1026, doi: 10.1021/ja01862a010.

Musgrove, M., 2000, Temporal links between climate and hydrology: Insights from central Texas caves and groundwater [Ph.D. thesis]: Austin, University of Texas, 432 p.

Musgrove, M., Banner, J.L., Mack, L.E., Combs, D.M., James, E.W., Cheng, H., and Edwards, R.L., 2001, Geochronology of late Pleistocene to Holocene speleothems from central Texas: Implications for regional paleoclimate: Geological Society of America Bulletin, v. 113, p. 1532–1543.

Niggemann, S., Mangini, A., Mudelsee, M., Richter, D.K., and Wurth, G., 2003a, Sub-Milankovitch climatic cycles in Holocene stalagmites from Sauerland, Germany: Earth and Planetary Science Letters, v. 216, p. 539–547, doi: 10.1016/S0012-821X(03)00513-2.

Niggemann, S., Mangini, A., Richter, D.K., and Wurth, G., 2003b, A paleoclimate record of the last 17,600 years in stalagmites from the B7 cave, Sauerland, Germany: Quaternary Science Reviews, v. 22, p. 555–567, doi: 10.1016/S0277-3791(02)00143-9.

Onac, B.P., Constantin, S., Lundberg, J., and Lauritzen, S.-E., 2002, Isotopic climate record in a Holocene stalagmite from Ursilor Cave (Romania): Journal of Quaternary Science, v. 17, p. 319–327, doi: 10.1002/jqs.685.

Parkhurst, D.L., and Appelo, C.A.J., 1999, User's guide to PHREEQC (version 2)—A computer program for speciation, reaction-path, 1D-transport, and inverse geochemical calculations: U.S. Geological Survey Water Resources Investigations Report 99-4259, p. 312.

Paulsen, D.E., Li, H.-C., and Ku, T.-L., 2003, Climate variability in central China over the last 1270 years revealed by high-resolution stalagmite records: Quaternary Science Reviews, v. 22, p. 691–701, doi: 10.1016/S0277-3791(02)00240-8.

Pazdur, A., Pazdur, M.F., Pawlyta, J., Górny, A., and Olszewski, M., 1995, Paleoclimatic implications of radiocarbon dating of speleothems from the Cracow-Wielún Upland, southern Poland: Radiocarbon, v. 37, p. 103–110.

Plagnes, V., Causse, C., Genty, D., Paterne, M., and Blamart, D., 2002, A discontinuous climatic record from 187 to 74 ka from a speleothem of the Clamouse Cave (south of France): Earth and Planetary Science Letters, v. 201, p. 87–103, doi: 10.1016/S0012-821X(02)00674-X.

Raich, J.W., and Schlesinger, W.H., 1992, The global carbon dioxide flux in soil respiration and its relationship to vegetation and climate: Tellus, ser. B, Chemical and Physical Meteorology, v. 44, p. 81–99.

Repinski, P., Holmgren, K., Lauritzen, S.E., and Lee-Thorp, J.A., 1999, A late Holocene climate record from a stalagmite, Cold Air Cave, Northern Province, South Africa: Palaeogeography, Palaeoclimatology, Palaeoecology, v. 150, p. 269–277, doi: 10.1016/S0031-0182(98)00223-5.

Romanek, C.S., Grossman, E.L., and Morse, J.W., 1992, Carbon isotope fractionation in synthetic aragonite and calcite: Effects of temperature and precipitation rate: Geochimica et Cosmochimica Acta, v. 56, p. 419–430, doi: 10.1016/0016-7037(92)90142-6.

Rozanski, K., Araguás-Araguás, L., and Gonfiantini, R., 1993, Isotopic patterns in modern global precipitation, *in* Swart, P.K., et al., eds., Climate change in continental isotope records: American Geophysical Union Geophysical Monographs, p. 1–36.

Schwarcz, H.P., 1986, Geochronology and isotopic geochemistry of speleothems, *in* Fritz, P., and Fontes, J.C., eds., Handbook of environmental isotope geochemistry—The terrestrial environment B: Amsterdam, Elsevier, p. 271–303.

Schwehr, K.A., 1998, Oxygen isotopic variations of soda straw cave deposits from the Yucatan Peninsula: A test of their use as a paleoprecipitation tool [M.S. thesis]: Houston, University of Houston, 180 p.

Serefiddin, F., Schwarcz, H.P., Ford, D.C., and Baldwin, S., 2004, Late Pleistocene paleoclimate in the Black Hills of South Dakota from isotope records in speleothems: Palaeogeography, Palaeoclimatology, Palaeoecology, v. 203, p. 1–17, doi: 10.1016/S0031-0182(03)00639-4.

Spötl, C., and Mangini, A., 2002, Stalagmite from the Austrian Alps reveals Dansgaard-Oeschger events during isotope stage 3: Implications for the absolute chronology of Greenland ice cores: Earth and Planetary Science Letters, v. 203, p. 507–518, doi: 10.1016/S0012-821X(02)00837-3.

Spötl, C., Burns, S.J., Mangini, A., and Frank, N., 2002, Stable isotopes in speleothems as proxies of past environmental changes in the Alps, *in* Proceedings of Study of environmental change using isotope techniques: Vienna, International Atomic Energy Agency, p. 286–291.

Stowe, L.G., and Teeri, J.A., 1978, The geographic distribution of C4 species of the Dicotyledonae in relation to climate: American Naturalist, v. 112, p. 609–623, doi: 10.1086/283301.

Talma, A.S., and Vogel, J.C., 1992, Late Quaternary paleotemperatures derived from a speleothem from Cango Caves, Cape Province, South Africa: Quaternary Research, v. 37, p. 203–213, doi: 10.1016/0033-5894(92)90082-T.

Talma, A.S., Vogel, J.C., and Partridge, T.C., 1974, Isotopic contents of some Transvaal speleothems and their palaeoclimatic significance: South African Journal of Science, v. 70, p. 135–140.

Tan, M., Liu, D., Zhong, H., Qin, X., Li, H., Zhao, S., Li, T., Lu, J., and Lu, X., 1998, Preliminary study on climatic signals of stable isotopes from Holocene speleothems under monsoon condition: Chinese Science Bulletin, v. 43, p. 506–509.

Thompson, P., Schwarcz, H.P., and Ford, D.C., 1976, Stable isotope geochemistry, geothermometry, and geochronology of speleothems from West Virginia: Geological Society of America Bulletin, v. 87, p. 1730–1738, doi: 10.1130/0016-7606(1976)87<1730:SIGGAG>2.0.CO;2.

Treble, P.C., Chappell, J., Gagan, M.K., McKeegan, K.D., and Harrison, T.M., 2005, In situ measurement of seasonal $\delta^{18}O$ variations and analysis of isotopic trends in a modern speleothem from southwest Australia: Earth and Planetary Science Letters, v. 233, p. 17–32, doi: 10.1016/j.epsl.2005.02.013.

Tsai, W.-S., 2002, Preliminary study of strontium isotope in late Pleistocene speleothems in Taiwan [M.S. thesis]: Tainan, Taiwan, National Cheng Kung University, 84 p.

Usdowski, E., and Hoefs, J., 1993, Oxygen isotope exchange between carbonic acid, bicarbonate, carbonate, and water: A re-examination of the data of McCrea (1950) and an expression for the overall partitioning of oxygen isotopes between the carbonate species and water: Geochimica et Cosmochimica Acta, v. 57, p. 3815–3818, doi: 10.1016/0016-7037(93)90159-T.

Vaks, A., Bar-Matthews, M., Ayalon, A., Schilman, B., Gilmour, M., Hawkesworth, C.J., Frumkin, A., Kaufman, A., and Matthews, A., 2003, Paleoclimate reconstruction based on the timing of speleothem growth and oxygen and carbon isotope composition in a cave located in the rain shadow in Israel: Quaternary Research, v. 59, p. 182–193, doi: 10.1016/S0033-5894(03)00013-9.

van Beynen, P.E., Schwartz, H.P., and Ford, D.C., 2004, Holocene climatic variation recorded in a speleothem from McFail's Cave, New York: Journal of Cave and Karst Studies, v. 66, p. 20–27.

Verheyden, S., Keppens, E., Fairchild, I.J., McDermott, F., and Weis, D., 2000, Mg, Sr and Sr isotope geochemistry of a Belgian Holocene speleothem: Implica-

tions for paleoclimate reconstructions: Chemical Geology, v. 169, p. 131–144, doi: 10.1016/S0009-2541(00)00299-0.

Wang, X., 1986, U-dating and $\delta^{18}O$, $\delta^{13}C$ features of speleothems in Maomaotou Big Cave: Guilin: Kexue Tongbao, v. 31, p. 835–838.

Wang, Y., Chen, Q., Liu, Z., Chen, Y., Zhou, C., and Lu, C., 1998, A continuous 200-ka palaeoclimate record from a stalagmite in Tangshan Cave, Nanjing: Chinese Science Bulletin, v. 43, p. 233–237.

Wang, Y., Wu, J., Xu, H., and Mu, X., 2000, Palaeoclimatic and environmental significance as indicated by the stable isotopic composition of cave stalagmite in Tangshan, Nanjing: Di zhi xue bao (Acta Geologica Sinica, Chinese Edition), v. 74, p. 333–338.

Wang, Y.J., Cheng, H., Edwards, R.L., An, Z.S., Wu, J.Y., Shen, C.-C., and Dorale, J.A., 2001, A high-resolution absolute-dated late Pleistocene monsoon record from Hulu Cave, China: Science, v. 294, p. 2345–2348, doi: 10.1126/science.1064618.

Wang, Z., Huang, P., Peng, Z., Yang, H., Jin, S., Liang, R., Zhang, H., and Quan, Y., 1995, ESR and U series dating of stalagmites and isotope paleoclimatology: Earth Science—Journal of China University of Geosciences, v. 20, p. 677–681.

Wang, Z., Zhi, X., and Zhang, H., 1997, Study by stable isotope method on for stalagmite from Hangzhou area: Acta Sedimentologica Sinica, v. 15, p. 77–79.

Williams, P.W., Marshall, A., Ford, D.C., and Jenkinson, A.V., 1999, Palaeoclimatic interpretation of stable isotope data from Holocene speleothems of the Waitomo District, North Island, New Zealand: The Holocene, v. 9, p. 649–657, doi: 10.1191/095968399673119429.

Williams, P.W., King, D.N.T., Zhao, J.-X., and Collerson, K.D., 2004, Speleothem master chronologies: Combined Holocene $^{18}O$ and $^{13}C$ records from the North Island of New Zealand and their palaeoenvironmental interpretation: The Holocene, v. 14, p. 194–208, doi: 10.1191/0959683604hl676rp.

Wurth, G., Niggemann, S., Richter, D.K., and Mangini, A., 2004, The Younger Dryas and Holocene climate record of a stalagmite from Hölloch Cave (Bavarian Alps, Germany): Journal of Quaternary Science, v. 19, p. 291–298, doi: 10.1002/jqs.837.

Xia, J., Engstrom, D.R., and Ito, E., 1997, Geochemistry of ostracode calcite: 2. Effects of the water chemistry and seasonal temperature variation on *Candona rawsoni:* Geochimica et Cosmochimica Acta, v. 61, p. 383–391, doi: 10.1016/S0016-7037(96)00354-7.

Xia, Q., Zhao, J.-x., and Collerson, K.D., 2001, Early–Mid Holocene climatic variations in Tasmania, Australia: Multi-proxy records in a stalagmite from Lynds Cave: Earth and Planetary Science Letters, v. 194, p. 177–187, doi: 10.1016/S0012-821X(01)00541-6.

Yadava, M.G., and Ramesh, R., 2005, Monsoon reconstruction from radiocarbon dated tropical Indian speleothems: The Holocene, v. 15, p. 48–59, doi: 10.1191/0959683605h1783rp.

Yadava, M.G., Ramesh, R., and Pant, G.B., 2004, Past monsoon rainfall variations in peninsular India recorded in a 331-year-old speleothem: The Holocene, v. 14, p. 517–524, doi: 10.1191/0959683604hl728rp.

Yuan, D., Cheng, H., Edwards, R.L., Dykoski, C.A., Kelly, M.J., Zhang, M., Qing, J., Lin, Y., Wang, Y., Wu, J., Dorale, J.A., An, Z., and Cai, Y., 2004, Timing, duration, and transitions of the last interglacial Asian monsoon: Science, v. 304, p. 575–578, doi: 10.1126/science.1091220.

Zhang, J., Quay, P.D., and Wilbur, D.O., 1995, Carbon isotope fractionation during gas-water exchange and dissolution of $CO_2$: Geochimica et Cosmochimica Acta, v. 59, p. 107–114, doi: 10.1016/0016-7037(95)91550-D.

Zhang, M., Yuan, D., Lin, Y., Cheng, H., Qin, J., and Zhang, H., 2004a, The record of paleoclimatic change from stalagmites and the determination of termination II in the south of Guizhou Province, China: Science in China, Ser. D, v. 47, p. 1–12.

Zhang, M., Yuan, D., Lin, Y., Qin, J., Li, B., Cheng, H., and Edwards, R.L., 2004b, A 6000-year high-resolution climatic record from a stalagmite in Xiangshui Cave, Guilin, China: The Holocene, v. 14, p. 697–702, doi: 10.1191/0959683604hl748rp.

Zhao, J.-x., Wang, Y.-j., Collerson, K.D., and Gagan, M.K., 2003, Speleothem U-series dating of semi-synchronous climate oscillations during the last deglaciation: Earth and Planetary Science Letters, v. 216, p. 155–161, doi: 10.1016/S0012-821X(03)00501-6.

Manuscript Received by the Society 9 August 2004
Revised Manuscript Received 28 February 2005
Manuscript Accepted 3 May 2005

Printed in the USA